GMD-2020-323 by Wang et al.

Responses to Reviewer(s)

Apr. 1, 2021

Response to Reviewer #3

Interactive comment on "The GPU version of LICOM3 under the HIP framework and its large-scale application" by Wang et al. (2020).

Anonymous Referee #3

Received: 30 Mar. 2021

The paper describes the GPU parallelization of LICOM3, good parallel speed ups and good scalability toward a large number of GPUs has been obtained. The paper focusses on GPU programming and code optimization rather than model development (in this case scope ocean model). However, given the scope of the journal, I would advise to include some introduction of components/program modules of LICOM3 in terms of ocean dynamics. Furthermore, there are too many inaccurate or incorrect language usage, the paper needs to be corrected by a native English speaker.

Response: Thanks for your comments and suggestions. Following your suggestions, we have added some descriptions in Section 2.1 to introduce the components and program modules of LICOM3 briefly as follows, particularly for the seven subroutines porting to GPU. We have further revised the English of the manuscript and have ask a professional English editor to polish it. The editing certification is included at the end of this letter. The point-to-point responses are listed as follows.

"*The essential task of the ocean model is to solve the approximated Navier-Stocks equations, along with the conservation equations of the temperature and salinity. Seven kernels are within the time integral loop, named "readyt", "readyc", "barotr", "bclinc", "tracer", "icesnow", and "convadj", which are also the main subroutines porting from the CPU to the GPU. The former two kernels computed the terms in the barotropic and baroclinic equations of the model. The following three ("barotr", "bclinc", and "tracer") are used to solve the barotropic, baroclinic, and temperature/salinity equations. The last*

two subroutines deal with the seaice and the deep convection processes at the high latitudes. All these subroutines have about 12000 lines of source code, accounting for approximately 25% of the total code and 95% of computation."

Detailed comments/questions:

Figure 5, Super linear speed ups are observed for some tracer and readyc from 384 to 768 GPUs. What are the reasons?

Response: Thanks. The speed of the model (also individual subroutines) not only depends on the number of cores but also on the speed of communication or the usage of memory/cache, particularly for the stencil problem in the present study. Based on our analysis, the kernels' (tracer and readyc) superlinear speedups are mainly caused by memory usage. That is, the memory usage of each thread for 768 GPU cards is only half for 384 GPU cards. That may cause the superlinear speedups.

Section 6. Conclusions contains many detailed discussions, the detailed discussions should be in 5. Discussion, and only briefly summarize the main conclusions in 6.

Response: Thank you very much for your suggestion. This is also what we had thought about when we wrote the paper. Because the discussions in Section 6 were a little scattered and seem to be closely related to the conclusions, we didn't put these discussions in Section 5. Also, further development of the model is discussed here. To make the manuscript much clearly, we do not move these discussions.

Line 16, explain "3-dimensional parallelization"

Response: Thanks. When solving the ocean circulation equations numerically, the seawater is used to discrete to a 3-dimensional grid (x, y and z). Usually, the grid has been horizontally partitioned into latitude belts (y direction) or longitude-latitude boxes (x and y direction) for parallelization. Here, "3-dimensional parallelization" means the grid has also been partitioned in the depth (or z direction) direction. We have added the explanation in the revised manuscript.

Line 69, model's best computing performance? Do you mean only the best or fastest results are reported?

Response: Yes. Only the best or fastest results are reported. Because several other users were also conducting tests when we run ours. Therefore, the results may be affected by the other jobs. We think that the best or fastest results may reflect the actual ability of the machine.

Line 160, What are "GPU space nodes"?

Response: Thanks. “GPU space nodes” are confusing. We actually want to say “GPU memory spaces at different nodes”. We modified it in the revised manuscript.

Line 169, What is “Ocean block distribution”? Describe.

Response: Thanks. “Ocean block distribution” means to distribute the data on the partitioned grid to each thread. We revised this expression in the manuscript.

Line 170, The description is too much in terms of code execution steps (loops). Describe tracer, barocline and barotropic in terms of sub-models of ocean dynamics.

Response: Thanks. We have been added brief descriptions of seven kernels in the revised manuscript in Section 2.1. You also suggested this at the beginning of your comments.

Line 179,” The results are the time running one model month”, do you mean: The time reported is the wall clock time of running one model month?

Response: Thanks. Yes, it is. We changed it to “The results are the wall clock time of running one model month”.

Line 214, “the 3-D parallelism is implemented”, what is 3-D parallelism? please elaborate

Response: Thanks. “the 3-D parallelism” is actually “the 3-dimensional parallelism”. When solving the ocean circulation equations numerically, the seawater is used to discrete to a 3-dimensional grid (x, y, and z). Usually, the grid has been horizontally partitioned into latitude (or y) belts or longitude-latitude (or x-y) boxes for parallelization on CPU or GPU. Here, “3-dimensional parallelization” means the grid has also been partitioned in the depth (or z) direction. Initially, the LICOM3 are using only 2-D MPI parallelism in the x and y directions. To increase the scalability of the HIP version, we also partitioned the grid in the z-direction. We further explained this term in the revised manuscript.

Line 259, “equivalent to one step”, one step of what?

Response: Thanks. We want to express that the data reading time is comparable to the wall clock time for one model step. We modified it in the revised manuscript.

Line 261, “we then rewrite the data reading strategy and do parallel scattering for ten different forcing variables”, needs more explanation.

Response: Thanks. We decreased the reading frequency from every day to every month but using large arrays for the input. Originally, 10 variables are sequentially read from 10 files, interpolated to 1/20°grid and then scattered to each processor or thread. All the processes are done at the master processor. In the revised code, we use 10 different processes to read, interpolate and scatter parallelly, hence reduce the time to about 1/10 of the original. We will explain this in the revised manuscript.

Line 263, What is “the core-process”?

Response: Thanks. The core-process here indicated the computation routines within one integration step, and it does not include the daily-mean and I/O. We further revised the expression in the manuscript.

Line 389, What are “The dynamic core and physic packages”?

Response: Thanks. The former, the dynamic core, is the code to solve the equations numerically. The latter, the physic packages, is the code to compute the contributions of physic processes to the change of the circulation. Usually, these two parts are coded separately in the oceanic or atmospheric general circulation models. We further revised the expression in the manuscript.

Some minor corrections:

Line 20, Change “can still obtain an increasing,” to “can still be increased to”

Line 60, Change “is supported by” to “provides support for”

Line 81, Change “preparing” to “in preparation”

Line 109, Change “totally” to “in total,”

Line 111, grammar

Line 112, Change “are suitable for” to “require” or “demand”

Line 154, Remove “including”

Line 164, Change “earlier” to “ago”

Line 196, Change “grids were united “ to “grid points are grouped”

Line 217, “parallel” to “parallelize”

Line 223, “parallel” to “parallelization”

Line 245, “Variable” to “Floating point” or “Arithmetic”

Line 259, “updated” to “increased”

Line 269, Change “0.2-0.3 SYPD will require too much” to “at a speed of 0.2-0.3 SYPD it will take too long”

Response: Done. Many thanks for your help in improving the language of the manuscript. All the improper usages have been corrected in the revised manuscript following your suggestions.

Editing Certificate

This document certifies that the manuscript

The GPU version of LICOM3 under the HIP framework and its large-scale application

prepared by the authors

Pengfei Wang, Jinrong Jiang, Pengfei Lin, Mengrong Ding, Junlin Wei et al.

was edited for proper English language, grammar, punctuation, spelling, and overall style by one or more of the highly qualified native English speaking editors at AJE.

This certificate was issued on **April 7, 2021** and may be verified on the AJE website using the verification code **BFCC-ABAC-4B79-965A-D0E4** .

Neither the research content nor the authors' intentions were altered in any way during the editing process. Documents receiving this certification should be English-ready for publication; however, the author has the ability to accept or reject our suggestions and changes. To verify the final AJE edited version, please visit our verification page at aje.com/certificate. If you have any questions or concerns about this edited document, please contact AJE at support@aje.com.

AJE provides a range of editing, translation, and manuscript services for researchers and publishers around the world. For more information about our company, services, and partner discounts, please visit aje.com.

The GPU version of LICOM3 under the HIP framework and its large-scale application

Pengfei Wang[1,3], Jinrong Jiang[2, 4*], Pengfei Lin[1,4*], Mengrong Ding[1], Junlin Wei[2], Feng Zhang[2], Lian Zhao[2], Yiwen Li[1], Zipeng Yu[1], Weipeng Zheng[1,4], Yongqiang Yu[1,4], Xuebin Chi[2, 4] and Hailong Liu[1,4*]

[1]State Key Laboratory of Numerical Modeling for Atmospheric Sciences and Geophysical Fluid Dynamics (LASG), Institute of Atmospheric Physics (IAP), Chinese Academy of Sciences (CAS), Beijing 100029, China
[2]Computer Network Information Center, Chinese Academy of Sciences, Beijing 100190, China
[3]Center for Monsoon System Research (CMSR), Institute of Atmospheric Physics, Chinese Academy of Sciences, Beijing 100190, China
[4]University of Chinese Academy of Sciences, Beijing 100049, China

Correspondence: Drs. Jinrong Jiang [jjr@sccas.cn], Pengfei Lin [linpf@mail.iap.ac.cn] and Hailong Liu [lhl@lasg.iap.ac.cn]

Abstract. A high-resolution (1/20°) global ocean general circulation model with graphics processing unit (GPU) code implementations is developed based on the LASG/IAP Climate System Ocean Model version 3 (LICOM3) under a heterogeneous-compute interface for portability (HIP) framework. The dynamic core and physics package of LICOM3 are both ported to the GPU, and 3-dimensional parallelization (also partitioned in the vertical direction) is applied. The HIP version of LICOM3 (LICOM3-HIP) is 42 times faster than the same number of CPU cores when 384 AMD GPUs and CPU cores are used. LICOM3-HIP has excellent scalability; it can still obtain a speedup of more than four on 9216 GPUs compared to 384 GPUs. In this phase, we successfully performed a test of 1/20° LICOM3-HIP using 6550 nodes and 26200 GPUs, and on a large scale, the model's speed was increased to approximately 2.72 simulated years per day (SYPD). By putting almost all the computation processes inside GPUs, the time cost of data transfer between CPUs and GPUs was reduced, resulting in high performance. Simultaneously, a 14-year spin-up integration following phase 2 of the Ocean Model Intercomparison Project (OMIP-2) protocol of surface forcing was performed, and preliminary results were evaluated. We found that the model results had little difference from the CPU version. Further comparison with observations and lower-resolution LICOM3 results suggest that the 1/20° LICOM3-HIP can reproduce the observations and produce many smaller-scale activities, such as submesoscale eddies and frontal scale structures.

1 Introduction

Numerical models are a powerful tool for weather forecasts and climate prediction and projection. Creating high-resolution atmospheric, oceanic and climatic models remains a significant scientific and engineering challenge because of the enormous computing, communication, and input/output (IO) involved. Kilometer-scale weather and climate simulation have recently started to emerge (Schär et al., 2020). Due to the considerable increase in computational cost, such models will only work with extreme-scale high-performance computers and new technologies.

Deleted:
Deleted: *to*
Deleted: Graphics
Deleted: units (GPUs
Deleted: system
Deleted: Heterogeneous
Deleted: Interface
Deleted: Portability
Deleted: the
Deleted: The
Deleted: comparing
Deleted: at the grand
Deleted: time
Deleted: solution can still obtain an increasing, about
Deleted: The high performance was due to
Deleted: of
Deleted: reducing
Deleted: has been conducted
Deleted: the
Deleted: have been
Deleted: have
Deleted: suggests
Deleted: scales
Deleted: High
Deleted: ocean
Deleted: climate
Deleted: remain
Deleted: challenges
Deleted: start
Deleted: recently
Deleted: tremendous
Deleted: computation

Global ocean general circulation models (OGCMs) are a fundamental tool for oceanography research, ocean forecasting, and climate change research (Chassignet et al., 2019). Such model performance is determined mainly by model resolution and subgrid parameterization and surface forcing. The horizontal resolution of global OGCMs has increased to approximately 5-10 km, which is also called eddy-resolving models. Increasing the resolution will significantly improve the simulation of western boundary currents, mesoscale eddies, fronts and jets, and currents in narrow passages (Hewitt et al., 2017). Meanwhile, the ability of an ocean model to simulate the energy cascade (Wang et al., 2019), the air-sea interaction (Hewitt et al., 2017), and the ocean heat uptake (Griffies et al., 2015) will be improved with increasing resolution. All these factors will effectively improve ocean model performance in the simulation and prediction of ocean circulation. Additionally, the latest numerical and observational results show that much smaller eddies (submesoscale eddies with a spatial scale of approximately 5-10 km) are crucial to vertical heat transport in the upper-ocean mixed layer and significant to biological processes (Su et al., 2018). Resolving the smaller-scale processes raises a new challenge for the horizontal resolution of OGCMs, which also demands much more computing resources.

Heterogeneous computing has become a development trend of high-performance computers. In the latest TOP500 supercomputer list released in November 2020, central processing unit (CPU) and graphic processing unit (GPU) heterogeneous machines account for six of the top 10. After the NVIDIA Corporation provided supercomputing techniques on GPUs, an increasing number of ocean models applied these high-performance acceleration methods to conduct weather or climate simulations. Xu et al. (2015) developed POM.gpu, a full GPU solution based on mpiPOM on a cluster, and achieved a 6.8 times energy reduction. Yashiro et al. (2016) deployed the NICAM model on the TSUBAME supercomputer, and the model sustained a double-precision performance of 60 T Flops on 2560 GPUs. Yuan et al. (2020) developed a GPU version of a wave model with 2 V100 cards and obtained a speedup of 10-12 times when compared to the 36 cores of the CPU. Yang et al. (2016) implemented a fully implicit β-plane dynamic model with a 488 m grid spacing on the TaihuLight system and achieved 7.95P Flops. Fuhrer et al. (2018) reported a 2-km regional atmospheric general circulation model (AGCM) test using 4888 GPU cards and obtained simulation performance for 0.043 simulated years per wall clock day (SYPD). Zhang et al. (2020) successfully ported a high-resolution (25 km atmosphere and 10 km ocean) Community Earth System Model in the TaihuLight supercomputer and obtained 1-3.4 SYPD.

Additionally, the AMD company also provides GPU solutions. In general, AMD GPUs use heterogeneous compute compiler (HCC) tools to compile codes, and they cannot use the compute unified device architecture (CUDA) development environments, which provide support for the NVIDIA GPU only. Therefore, due to the wide use and numerous CUDA learning resources, AMD developers must study two kinds of GPU programming skills. AMD's heterogeneous-compute interface for portability (HIP) is an open-source solution to address this problem. It provides a higher-level framework to contain these two types of lower-level development environments, i.e., CUDA and HCC, simultaneously. The HIP code's grammar is similar to that of the CUDA code, and with a simple conversion tool, the code can be compiled and run at CUDA and AMD architects, HCC/OpenACC is more convenient for AMD GPU developers than the HIP, which is popular from the coding viewpoint.

Deleted: The global…lobal ocean general circulation models (OGCMs) are a fundamental tool for oceanography research, ocean forecast…orecasting, and climate change research (Chassignet et al., 2019). Such models'…odel performance is determined mainly by model resolution and sub-grid…ubgrid parameterization,…and surface forcing. The horizontal resolution of global OGCMs has increased to about…pproximately 5-10 km, which is also called resolving models. The increasing…ncreasing the resolution will significantly improve the simulation of the …estern boundary currents, mesoscale eddies, fronts and jets, and the …urrents in narrow passages (Hewitt et al., 2017). Meanwhile, the ability of an ocean model in simulating…o simulate the energy cascade (Wang et al., 2019), the air-sea interaction (Hewitt et al., 2017), and the ocean heat uptake (Griffies et al., 2015) will be improved with the …ncreasing resolution. All these factors will effectively improve ocean models'…odel performance in the simulation and prediction of the …cean circulation. Additionally, the latest numerical and observational results show that the …uch smaller eddies (sub-mesoscale…ubmesoscale eddies with a spatial scale of about…pproximately 5-10 km) are crucial to the …ertical heat transport in the upper-ocean mixed layer and also …ignificant to biological processes (Su et al., 2018). To resolve ... [1]

Deleted: Nov….ovember 2020, Central Processing Unit…entral processing unit (CPU) and Graphics Processing Unit…raphic processing unit (GPU) heterogeneous machines account for six of the top 10. After the NVIDIA Corporation provided the …upercomputing technics…echniques on GPU, more and more…PUs, an increasing number of ocean models applied these high-performance acceleration ways…ethods to conduct weather or climate simulations. Xu et al. (2015) developed POM.gpu, a full GPU solution based on the …piPOM on a cluster, and gained…chieved a 6.8 times energy reduction. Yashiro et al. (2016) deployed the NICAM model on the TSUBAME supercomputer, and the model sustained a double-precision performance of 60T…0 T Flops on 2560 GPUs. Yuan et al. (2020) developed a GPU version of a wave model with 2 V100 cards and obtained a speedup of 10-12 times speedup than…hen compared to the 36 cores of the CPU. Yang et al. (2016) implemented a fully implicit β-plane dynamic model with 488m…488 m grid spacing on the TaihuLight system and achieving…chieved 7.95P Flops. Fuhrer et al. (2018) reported a 2-km regional Atmospheric General Circulation Model…tmospheric general circulation model (AGCM) test using 4888 GPU cards and obtained simulation performance for 0.043 simulated years per wall clock day (SYPD). Zhang et al. (2020) successfully ported a hi ... [2]

Deleted: At the same time…dditionally, the AMD company also provides its …PU solutions. In general, AMD GPU uses Heterogeneous Compute Compiler…PUs use heterogeneous compute compiler (HCC) tools to compile codes;… and they cannot use the Compute Unified Device Architecture…ompute unified device architecture (CUDA) development environments, which is supported by …rovide support for the NVIDIA GPU only. Therefore, due to the wildly used…ide use and numerous CUDA learning resources, AMD developers have to…ust study two kinds of GPU programming skills. AMD's Heterogeneous…eterogeneous-compute Interface…nterface for Portability…ortability (HIP) is an open-source solution to deal with…ddress this problem. It provides a higher-level framework to contain these two types of lower-level development environments, i.e., CUDA and HCC, simultaneously. The HIP code's grammar is like…imilar to that of the CUDA code, and with a simple convert…onversion tool, the code can be compiled and run at CUDA and AMD architects, respectively. The… HCC/OpenACC is more convenient for AMD GPU developers before ... [3]

Another reason is that CUDA GPUs currently have more market share. It is believed that an increasing number of codes will be ported to the HIP in the future. However, almost no ocean models use the HIP framework to date.

This study aims to develop a high-performance OGCM based on LICOM3, which can be run on an AMD GPU architecture using the HIP framework. Here, we will focus on the model's best or fastest computing performance and its practical usage for research and operation purposes. Section 2 is the introduction of the LICOM3 model. Section 3 contains the main optimization of LICOM3 under HIP. Section 4 covers the performance analysis and model verification. Section 5 is a discussion, and the conclusion is presented in Section 6.

2 The LICOM3 model and experiments

2.1 The LICOM3 model

In this study, the targeting model is the LASG/IAP Climate System Ocean Model version 3 (LICOM3), which was developed in the late 1980s (Zhang and Liang, 1989). Currently, LICOM3 is the ocean model for two air-sea coupled models of CMIP6, the Flexible Global Ocean-Atmosphere-Land System model version 3 with a finite-volume atmospheric model (FGOALS-f3; He et al., 2020) and the Flexible Global Ocean-Atmosphere-Land System model version 3 with a grid-point atmospheric model (CAS FGOALS-g3; Li et al., 2020). LICOM version 2 (LICOM2.0, Liu et al., 2012) is also the ocean model of the CAS Earth System Model (CAS-ESM, Zhang, et al., 2020). A future paper to fully describe the new features and baseline performances of LICOM3 is in preparation.

In recent years, the LICOM model was substantially improved based on LICOM2.0 (Liu et al., 2012). There are three main aspects. First, the coupling interface of LICOM has been upgraded. Now, NCAR flux coupler version 7 is employed (Lin et al., 2016), in which memory usage has been dramatically reduced (Craig et al., 2012). This makes the coupler suitable for application to high-resolution modeling.

Second, both orthogonal curvilinear coordinates (Murray, 1996; Madec & Imbard, 1996) and tripolar grids have been introduced in the LICOM. Now, the two poles are at (65°E, 60.8°N) and (115°W, 60.8°N) for the 1° model, at (65°E, 65°N) and (115°W, 65°N) for the 0.1° model, and at (65°E， 60.4°N) and (115°W, 60.4°N) for the 1/20° model of the LICOM. After that, the zonal filter in high latitudes, particularly in the Northern Hemisphere, was eliminated, which significantly improved the scalability and efficiency of the parallel algorithm of the LICOM3 model. In addition, the dynamic core of the model has also been updated accordingly (Yu et al., 2018), including application of a new advection scheme for the tracer formulation (Xiao, 2006) and addition of a vertical viscosity for the momentum formulation (Yu et al., 2018).

Third, the physical package has been updated, including introducing an isopycnal and thickness diffusivity scheme (Ferreira et al., 2005) and vertical mixing due to internal tides breaking at the bottom (St. Laurent et al., 2002). The coefficient of both isopycnal and thickness diffusivity is set to 300m^2 s^{-1} as the depth is either within the mixed layer or the water depth is shallower than 60 m. The upper and lower boundary values of the coefficient are 2000 and 300 m^2 s^{-1}, respectively.

Deleted: GPU has
Deleted: in the present.
Deleted: more and more
Deleted: so far
Deleted: The
Deleted: the
Deleted: optimizing
Deleted: the
Deleted: the
Deleted: for
Deleted: conclusions are
Deleted: system
Deleted: has been
Deleted: Now the
Deleted: the
Deleted: The
Deleted: The
Deleted: are preparing
Deleted: the
Deleted: :
Deleted: the
Deleted: the
Deleted: It
Deleted:
Deleted: to be applied
Deleted:
Deleted: the
Deleted: coordinate
Deleted: the
Deleted: grid
Deleted: the
Deleted: latitude
Deleted: northern hemisphere, has been
Deleted: improves
Deleted: applying
Deleted: the

Additionally, the chlorophyll-dependent solar shortwave radiation penetration scheme of Ohlmann (2003), the isopycnal mixing scheme (Redi, 1982; Gent & McWilliams, 1990), and the vertical viscosity and diffusivity schemes (Canuto et al. 2001; 2002) are employed in LICOM3.

Both the low-resolution (1°; Lin et al., 2020) and high-resolution (1/10°; Li Y. et al., 2020) stand-alone LICOM3 are also involved in OMIP-1 and OMIP-2; their outputs can be downloaded from websites. The two versions of LICOM3's performances compared with other CMIP6 ocean models are shown in Tsujino et al. (2020) and Chassignet et al. (2020). The 1/10° version has also been applied to perform short-term ocean forecasts (Liu et al., 2021).

The essential task of the ocean model is to solve the approximated Navier-Stocks equations, along with the conservation equations of the temperature and salinity. Seven kernels are within the time integral loop, named "readyt", "readyc", "barotr", "bclinc", "tracer", "icesnow", and "convadj", which are also the main subroutines porting from the CPU to the GPU. The former two kernels computed the terms in the barotropic and baroclinic equations of the model. The following three ("barotr", "bclinc", and "tracer") are used to solve the barotropic, baroclinic, and temperature/salinity equations. The last two subroutines deal with seaice and deep convection processes at high latitudes. All these subroutines have approximately 12000 lines of source code, accounting for approximately 25% of the total code and 95% of computation.

2.2 Configurations of the models

To investigate the GPU version, we employed three configurations in the present study. They are 1°, 0.1°, and 1/20°. Details of these models are listed in Table 1. The number of horizontal grid points for the three configurations are 360×218, 3600×2302, and 7200×3920. The vertical levels for the low-resolution models are 30, while they are 55 for the other two high-resolution models. From 1° to 1/20°, the computational effort increased by approximately 8000 (20^3) times (considering 20 times to decrease the time step), and the vertical resolution increased from 30 to 55, in total, approximately 15000 times. The original CPU version of 1/20° with MPI parallel on Tianhe-1A only reached 0.31 SYPD using 9216 CPU cores. This speed will slow down the 10-year spin-up simulation of LICOM3 to more than one month, which is not practical for climate research. Therefore, such simulations require extreme-scale high-performance computers by applying the GPU version.

In addition to the different grid points, three main aspects are different among the three experiments, particularly between version 1° and the other two versions. First, the horizontal viscosity schemes are different: using Laplacian for 1° and biharmonic for 1/10° and 1/20°. The viscosity coefficient is one order of magnitude smaller for the 1/20° version than for the 1/10° version, namely, -1.0×10^9 m^4/s for 1/10° vs -1.0×10^8 m^4/s for 1/20°. Second, although the force including dataset (JRA55-do; Tsujino et al., 2018) and the bulk formula for the three experiments are all standard of the OMIP-2, the periods and temporal resolutions of the forcing fields are different: 6-hour data from 1958 to 2018 for the 1° version, and daily mean data in 2016 for both the 1/10° and 1/20° versions. Third, version 1° is coupled with a sea ice model of CICE4 via NCAR flux coupler version 7, while the two higher-resolution models are stand-alone, without a coupler or sea ice model. Additionally,

Deleted: depended
Deleted:) (
Deleted:) (
Deleted: the
Deleted:), respectively.
Formatted: Font color: Text 1
Deleted: do
Formatted: Font color: Text 1
Deleted: 2020, under review
Formatted: Font color: Text 1
Deleted: have
Deleted: numbers
Deleted: , respectively.
Deleted: it increases
Deleted: about
Deleted: the
Deleted: for decreasing
Deleted: plus
Deleted: increase
Deleted: totally
Deleted: are suitable for
Deleted: Besides
Deleted: 1°
Formatted: Font: Symbol
Formatted: Font: Symbol
Formatted: Font: Symbol
Formatted: Font: Symbol
Formatted: Font: Symbol
Formatted: Font: Symbol
Formatted: Font: Symbol
Deleted: forcing
Formatted: Font: Symbol
Deleted: only
Formatted: Font: Symbol
Formatted: Font: Symbol
Deleted: the 1°
Deleted: the
Deleted: ,
Deleted: 's

the two higher-resolution experiments employ the new HIP version of LICOM3 (i.e., LICOM3-HIP); the low-resolution experiment does not employ this, including the CPU version of LICOM3 and the version submitted to OMIP (Lin et al., 2020). We also listed all the important information in Table 1, such as bathymetry data and the bulk formula, though these items are similar in the three configurations.

The spin-up experiments for the two high-resolution versions are conducted for 14 years, forced by the daily JRA55-do dataset in 2016. The atmospheric variables include the wind vectors at 10 m, air temperature at 10 m, relative humidity at 10 m, total precipitation, downward shortwave radiation flux, downward longwave radiation flux, and river runoff. According to the kinetic energy evolution, the models reach a quasi-equilibrium state after more than ten years of spin-up. The daily mean data are output for storage and analysis.

2.3 Hardware and software environments of the testing system

The two higher-resolution experiments were performed on a heterogeneous Linux cluster supercomputer located at the Computer Network Information Center (CNIC) of the CAS, China. This supercomputer consists of 7200 nodes (6 partitions or rings, each partition has 1200 nodes), with a 1.9 GHz X64 CPU of 32 cores on each node. Additionally, each node is equipped with four gfx906 AMD GPU cards with 16 GB memory. The GPU has 64 cores, for a total of 2560 threads on each card. The nodes are interconnected through high-performance InfiniBand (IB) networks (3-level fat-tree architecture using Mellanox 200 Gb/s HDR InfiniBand, whose measured point-to-point communication performance is approximately 23 GB/s). OpenMPI version 4.02 was employed for compiling, and the AMD GPU driver and libraries were rocm-2.9, integrated with HIP version 2.8. The storage file system of the supercomputer is ParaStor300S with a 'parastor' file system, whose measured write and read performance is approximately 520 GB/s and 540 GB/s, respectively.

3 LICOM3 GPU code structure and optimization

3.1 Introduction to HIP on an AMD hardware platform

AMD's HIP is a C++ runtime API and kernel language. It allows developers to create portable applications that can be run on AMD accelerators and CUDA devices. The HIP provides an API for an application to leverage GPU acceleration for both AMD and CUDA devices. It is syntactically similar to CUDA, and most CUDA API calls can be converted by replacing the character "cuda" with "hip" (or "Cuda" with "Hip"). The HIP supports a strong subset of CUDA runtime functionality, and its open-source software is currently available on GitHub (https://rocmdocs.amd.com/en/latest/Programming_Guides/HIP-GUIDE.html).

Some supercomputers install NVIDIA GPU cards, such as P100 and V100, and some install AMD GPU cards, such as AMD VERG20. Hence, our HIP version LICOM3 can adapt and gain very high performance at different supercomputer centers, such as Tianhe-2 and AMD clusters. Our coding experience on an AMD GPU indicates that the HIP is a good choice for high-

Deleted:). The
Deleted: , which was
Deleted: the same as
Deleted: the
Deleted: etc.,
Deleted: -
Deleted: -
Deleted: -
Deleted: the
Deleted: the
Deleted: the
Deleted: store
Deleted: ,
Deleted: Also
Deleted: the
Deleted: 200Gb
Deleted: about 23GB
Deleted: The
Deleted: is
Deleted: are
Deleted: about 520GB/s
Deleted: 's
Deleted: in placing of
Deleted: by
Deleted: by
Deleted: like
Deleted: , etc..

performance model development. Meanwhile, the model version is easy to keep consistent in these two commonly used platforms. In the following sections, the successful simulation of LICOM3-HIP is confirmed adequate to employ HIP.

Figure 1 demonstrates the HIP implementations necessary to support different types of GPUs. In addition to the differences in naming and libraries, there are other differences between HIP and CUDA including the following: 1) AMD Graphics Core Next (GCN) hardware "warp" size = 64; 2) device and host pointers allocated by HIP API use flat addressing (unified virtual addressing is enabled by default); 3) dynamic parallelism is not currently supported; 4) some CUDA library functions do not have AMD equivalents; and 5) shared memory and registers per thread may differ between the AMD and NVIDIA hardware. Despite these differences, most of the CUDA codes in applications can be easily translated to the HIP and vice versa.

Technical supports of CUDA and HIP also have some differences. For example, CUDA applications have some CUDA-aware MPI to direct MPI communication between different GPU memory spaces at different nodes, but HIP applications have no such functions to date. Data must be transferred from GPU memory to CPU memory in order to exchange data with other nodes and then transfer data back to the GPU memory.

3.2. Core computation process of LICOM3 and C transitional version

We attempted to apply the LICOM on a heterogeneous computer approximately five years ago, cooperating with the NVIDIA Corporation. LICOM2 was adapted to NVIDIA P80 by OpenACC Technical (Jiang et al., 2019). That was a convenient implementation of LICOM2-gpu using 4 NVIDIA GPUs to achieve a 6.6 speedup compared to 4 Intel CPUs, but its speedup was not as good when further increasing the GPU number.

During this research, we started from the CPU version of LICOM3. The code structure of LICOM3 includes four steps. The first step is the model setup, which involves MPI partitioning and ocean data distribution. The second stage is model initialization, which includes reading the input data and initializing the variables. The third stage is integration loops, or the core computation of the model. Three explicit time loops, which are for tracer, baroclinic and barotropic steps, are in one model day. The outputs and final processes are included in the fourth step.

Figure 2 shows the flowchart of LICOM3. The major processes within the model time integration include baroclinic, barotropic, and thermohaline equations, which are solved by the leapfrog or Euler forward scheme. There are seven individual subroutines, such as "readyt", "readyc", "barotr", "bclinc", "tracer", "icesnow", and "convadj". When the model finishes one day's computation, the diagnostics and output subroutine will write out the predicted variables to files. The output files contain all the necessary variables to restart the model and for analysis.

To obtain high performance, it is more efficient to use the native GPU development language. In the CUDA development forum, both CUDA-C and CUDA-Fortran are provided; however, Fortran's support is not as efficient as that for C++. We plan to push all the core process codes into GPUs; hence, the seven significant subroutines' Fortran codes must be converted to HIP/C++. Due to the complexity and many lines in these subroutines (approximately 12000 lines of Fortran code) and to ensure that the converted C/C++ codes are correct, we rewrote them to C before finally converting them to HIP codes.

Deleted: to be
Deleted: Besides
Deleted: including
Deleted: ,
Deleted: space
Deleted: so far. We have to transfer data
Deleted: for exchanging
Deleted: them
Deleted: tried
Deleted: about
Deleted: earlier
Deleted: The
Deleted: technical
Deleted: so
Deleted: This time
Deleted: ; it
Deleted: partition
Deleted: block
Deleted: initialize
Deleted: using
Deleted: is more efficient
Deleted: good
Deleted: making sure
Deleted: be

A bit-reproducible climate model produces the same numerical results for a given precision, regardless of the choice of domain decomposition, the type of simulation (continuous or restart), compilers, and the architectures executing the model (i.e., the same hardware and software conduct the same result). The C transitional version (not fully C code, but the seven core subroutines) is bit reproducible with the F90 version of LICOM3 (the binary output data are the same under Linux with the "diff" command). We also tested the execution time. The Fortran and C hybrid version's speed is slightly faster (less than 10%) than the original Fortran code. Figure 3 shows a speed benchmark by LICOM3 for 100 km and 10 km running on an Intel platform. The results are the wall clock time of running one model month for a low-resolution test and one model day for a high-resolution test. The details of the platform are in the caption of Figure 3. The results indicate that we successfully ported these kernels from Fortran to C.

This C transitional version becomes the starting point of HIP/C++ codes and reduces the complexity of developing the HIP version of LICOM3.

3.3. Optimization and tuning methods in LICOM3-HIP

The unit of computation in LICOM3-HIP is a horizontal grid point. For example, 1/20° corresponds to 7200×3920 grids. For the convenience of MPI parallelism, the grid points are grouped as blocks; that is, if $Proc_x \times Proc_y$ MPI processes are used in the x and y directions, then each block has $B_x \times B_y$ grids, where $Proc_x \times B_x$=7200 and $Proc_y \times B_y$=3920. Each GPU process performs 2-dimensional (2-D) or 3-dimensional (3-D) computations in these $B_x \times B_y$ grids, which is similar to the MPI process. 2-D means that the grids are partitioned only in the horizontal directions, and 3-D includes also the depth or vertical direction. In practice, four lateral columns are added to B_x and B_y (two on each side, $imt=B_x+4$, $jmt=B_y+4$) for the halo. Table 2 lists the frequently used block definitions of LICOM3.

The original LICOM3 was written in F90. To adapt it to a GPU, we applied Fortran/C hybrid programming. As shown in Figure 2, the codes are kept using the F90 language before entering device-stepon and after stepon-out. The core computation processes within the stepons are rewritten using HIP/C. Data structures in the CPU space remain the same as the original Fortran structures. The data commonly used by F90 and C are then defined by extra C, including files and defined by "extern" type pointers in C syntax to refer to them. In the GPU space, newly allocated GPU global memories hold the arrival correspondence to those in the CPU space, and the HipMemcpy is called to copy them in and out.

Seven major subroutines (including their subrecurrent calls) are converted from Fortran to HIP. The seven subroutine call sequences are maintained, but each subroutine is deeply recoded in the HIP to obtain the best performance. The CPU space data are 2-D or 3-D arrays; in the GPU space, they are changed to 1-D arrays to improve the data transfer speed between different GPU subroutines.

The LICOM3-HIP is two-level parallelism, and each MPI process corresponds to an ocean block. The computation within one MPI process is then pushed into the GPU. The latency of the data copy between the GPU and CPU is one of the bottlenecks

Deleted: cores subroutine
Deleted: -
Deleted: the
Deleted: have
Deleted: , less than 10%.
Deleted: the
Deleted: 100km
Deleted: 10km
Deleted: have
Deleted: the
Deleted: grids were united
Deleted: ,
Deleted: does
Deleted: computation
Deleted: as
Deleted: does
Deleted: the
Deleted: by
Deleted: arrives
Deleted: sub-recurrent
Deleted: calls
Deleted: re-coded
Deleted: we change them
Deleted: , improving
Deleted:
Deleted: corresponding

for daily computation loops. All read-only GPU variables are allocated and copied at the initial stage to reduce the data copy time. Some datum copy is still needed in the stepping loop, e.g., MPI call in barotr.cpp.

The computation block in MPI (corresponding to 1 GPU) is a 3-D grid; in the HIP revision, 3-D parallelism is implemented. This change adds more parallel inside one block than the MPI solo parallelism (only 2-D). Some optimizations are needed to adapt to this change, such as increasing the global arrays to avoid data dependency. A demo for using a temporary array to parallelize the computation inside a block is shown in Figure 4. Figure 4a represents a loop of the original code in the *k* direction. Since the variable *v(i,j,k)* has a dependence on *v(i,j,k+1)*, it will cause an error when the GPU threads are parallel in the *k* direction. We then separate the variable into two HIP kernel computations. In the upper part of Figure 4b, a temporary array *vt* is used to hold the result of *f1()*, and it can be GPU threads that are parallel in the *k* direction. Then, at the bottom of Figure 4b, we use *vt* to perform the computations of *f2()* and *f3()*; this can still be GPU threads that are parallel in the *k* direction. Finally, this loop of codes is parallelized.

Parallelization in a GPU is similar to a shared-memory program; memory write conflicts occur in the subroutine "tracer" advection computation. We change the if-else tree in this subroutine; hence, the data conflicts between neighboring grids are avoided, making the 3-D parallelism successful. Moreover, in this subroutine, we use more operations to alternate the data movement to reduce the cache usage. Since the operation can be GPU thread parallelized and will not increase the total computation time, reducing the memory cache improves this subroutine's final performance.

A notable problem when the resolution is increased to 1/20° is that the total size of Fortran common blocks will be larger beyond 2 GB. This change will not cause abnormalities for C in the GPU space. However, if the GPU process references the data, the system call in HipMemcpy will cause compilation errors (perhaps due to the compiler limitation of the GPU compilation tool). We can change the original Fortran arrays' data structure from the "static" to the "allocatable" type in this situation. Since a GPU is limited to 16 GB GPU memory, the ocean block size in one block should not be too large. In practice, the 1/20° version starts from 384 GPUs (and is regarded as the baseline for speedup here); if the partition is smaller than that value, sometimes insufficient GPU memory errors will occur.

We found that the "tracer" is the most time-consuming subroutine for the CPU version (Figure 5). With the increase of CPU cores from 384 to 9216, the ratio of cost time for "tracer" is also increasing from 38% to 49%. "readyt" and "readyc" are computing-intensive subroutines. "Tracer" is both a computing-intensive and communication-intensive subroutine. "barotr" is a communication-intensive subroutine. The communication of "barotr" is 45 times more than that of "tracer" (Table 3). Computing-intensive subroutines can achieve good GPU speed, but communication-intensive subroutines will achieve poor performance. The superlinear speedups for "tracer" and "readyc" might be mainly caused by memory usage, in which the memory usage of each thread for 768 GPU cards is only half for 384 GPU cards.

We performed a set of experiments to measure the time cost of both halo update and memory copy in the HIP version (Figure 6). These two processes in the time integration are conducted in three subroutines: "barotr", "bclinc," and "tracer". The figure shows that "barotr" is the most time-consuming subroutine, and the memory copy dominates, which takes approximately 40% of the total time cost.

Deleted: data
Deleted:
Deleted: the
Deleted: extra
Deleted: of
Deleted: parallel
Deleted: can be found
Deleted: paralleled
Deleted: do
Deleted: it
Deleted: The parallel
Deleted: more like
Deleted: the
Deleted: threads
Deleted: bigger
Deleted: abnormal
Deleted: But
Deleted: occur
Deleted: It is
Deleted: should
Deleted: it
Deleted: the GPU memory
Deleted:
Deleted: tracer
Deleted: The computing
Formatted: Font color: Text 1
Deleted: the
Formatted: Font color: Text 1
Deleted: subroutine
Formatted: Font color: Text 1
Formatted: Font color: Text 1
Deleted: have done
Deleted: about
Formatted: Font color: Text 1
Deleted:
Formatted: Font color: Text 1

Data operations inside CPU (or GPU) memory are at least one order of magnitude faster than the data transfer between GPU and CPU through 16X PCI-e. Halo exchange at the MPI level is similar to POP (Jiang et al. 2019). We did not change these codes in the HIP version. The four blue rows and columns in Figure 7 demonstrate the data that need to be exchanged with the neighbors. As shown in Figure 7, in GPU space, we pack the necessary lateral data for halo operation from *imt*×*jmt* to 4(*imt*+*jmt*). This change reduces the HipMemcpy data size to (4/*imt*+4/*jmt*) of the original one. The larger that *imt* and *jmt* are, the less the transferred data are. At 384 GPUs, this change saves approximately 10% of the total computation time. The change is valuable for the HIP since the platform has no CUDA-aware MPI installed; otherwise, the halo operation can be done in the GPU space directly as done by POM.gpu (Xu et al., 2015). The test indicates that the method can decrease approximately 30% of the total wall clock time of "barotr" when 384 GPUs are used. However, we have not optimized other kernels so far because their performance is not as good as 384 GPUs when the GPU scale exceeds 10000. We keep it here as an option to improve the performance of 'barotr' at operational scales (i.e., GPU scales under 1536).

3.4. Model I/O optimization

Approximately 3 GB forcing data are read from the disk every model year, while approximately 60 GB daily mean predicted variables are stored to disk every model day. The time cost for reading daily forcing data from the disk increased to 200 s in one model day after the model resolution increased from 1° to 1/20°. This time is comparable to the wall clock time for one model step when 1536 GPUs are applied; hence, we must optimize the model for total speedup. The cause of low performance is daily data reading and scattering to all nodes every model day; we then rewrite the data reading strategy and perform parallel scattering for ten different forcing variables. Originally, 10 variables are read from 10 files, interpolated to 1/20° grid and then scattered to each processor or thread. All the processes are sequentially done at the master processor. In the revised code, we use 10 different processes to read, interpolate and scatter parallelly. Finally, the time cost of input is reduced to approximately 20 s, which is 1/10 of the original time cost (shown below).

As indicated, the time cost for one integration step (excluding the daily mean and I/O) is approximately 200 s using 1536 GPUs. One model day's output needs approximately 250 s; this is also beyond the GPU computation time for one step. We modify the subroutine to a parallel version, which decreases the data write time to 70 s on the test platform (this also depends on system I/O performance).

4 Model performance

4.1. Model performance in computing

Performing kilometer-scale and global climatic simulations is challenging (Palmer, 2014; Schär et al., 2020). As specified by Fuhrer et al. (2018), the SYPD is a useful metric to evaluate model performance for a parallel model (Balaji et al., 2017). Because a climate model often needs to run for at least 30-50 years for each simulation, at a speed of 0.2-0.3 SYPD, the time

Deleted: Variable
Deleted: in
Formatted ... [5]
Deleted: and
Formatted ... [4]
Formatted ... [6]
Deleted: The halo
Formatted ... [7]
Deleted: in
Deleted: have
Formatted ... [8]
Formatted ... [9]
Deleted: .
Formatted ... [10]
Formatted ... [11]
Deleted: is
Formatted ... [12]
Deleted: about
Formatted ... [13]
Deleted: does
Formatted ... [14]
Deleted: by about
Formatted ... [15]
Deleted: But
Formatted ... [16]
Deleted: 384GPUs'
Formatted ... [17]
Deleted: GPUs
Formatted ... [18]
Deleted: beyond
Deleted: just
Formatted ... [19]
Formatted ... [20]
Deleted: 3GB… GB forcing data are read from the disk ever ... [21]
Formatted ... [22]
Deleted: about
Formatted ... [23]
Deleted: one
Formatted ... [24]
Deleted: core-process
Formatted ... [25]
Deleted: about 200s…pproximately 200 s using 1536 GPUs. ... [26]
Deleted: simulation are…imulations is challenging (Palmer, ... [27]
Formatted ... [28]

will be too long to finish the experiment. The common view is that at least 1-2 SYPD is an adequate entrance for a realistic climate study. It also depends on the time scale in a climate study. For example, for the 10-20-year simulation, 1-2 SYPD seems acceptable, and for the 50-100-year simulation, 5-10 SYPD is better. The NCEP weather prediction system throughput standard is 8 minutes to finish one model day, equivalent to 0.5 SYPD.

Figure 8 illustrates the I/O performance of LICOM3-HIP, comparing the performances of computation processes. When the model applies 384 GPUs, the I/O costs 1/10 of the total simulation time (Figure 8a). When the scale increases to 9216 GPUs, the I/O time increases but is still smaller than the GPU's step time (Figure 8b). The improved LICOM3 I/O in total costs approximately 50-90 s (depending on scales), especially when the input remains stable (Figure 8c) while scaling increases. This optimization of I/O maintains that LICOM3-HIP 1/20° runs well at all practice scales for a realistic climate study. The I/O time was cut off from the total simulation time in the follow-up test results to analyze the purely parallel performance.

Figure 9 shows the roof-line model using the Stream-GPU and the LICOM program's measured behavioral data on a single computation node bound to one GPU card depicting the relationship between arithmetic intensity and performance floating point operations. The 100 km resolution case is employed for the test. The blue and gray oblique lines are the fitting lines related to the Stream-GPU program's behavioral data using 5.12e8 and 1e6 threads, respectively, both with a blocksize of 256, which attain the best configuration. For details, the former is approximately the maximum thread number restricted by GPU card memory, achieving the bandwidth limit to 696.52 GB/s. In comparison, the latter is close to the average number of threads in GPU parallel calculations used by LICOM, reaching a bandwidth of 344.87 GB/s on average. Here, we use the oblique gray line as a benchmark to verify the rationality of LICOM's performance, accomplishing an average bandwidth of 313.95 GB/s. Due to the large calculation scale of the entire LICOM program, the divided calculation grid bound to a single GPU card is limited by video memory; most kernel functions issue no more than 1.2e6 threads. As a result, the floating-point operation performance is slightly far from the oblique roof-line shown in Figure 9. In particular, the subroutine bclinc apparently strays off of the entire trend for including frequent 3d-array Halo MPI communications and much data transmission occurs between the CPU and GPU.

Figure 10 shows the SYPD at various parallel scales. The baseline (384) of GPUs could achieve a 42 time speedup than that of the same number of CPU cores. Sometimes, we also count the overall speedup, 384 GPUs in 96 nodes versus the total 3072 CPU cores in 96 nodes. We can obtain an overall performance speedup of 384, or approximately 6-7 times. The figure also indicates that for all scales, the SYPD continues to increase. On the scale of 9216 GPUs, the SYPD first goes beyond 2, which is seven times the same CPU result. A quasi-whole machine (26200 GPUs, 26200×65=1703000 cores in total, one process corresponds to one CPU core plus 64 GPU cores) result indicates that it can still obtain an increasing SYPD to 2.72.

Since each node has 32 CPU cores and 4 GPUs, each GPU is managed by one CPU thread in the present cases. We can also quantify GPUs' speedup vs. all CPU cores' on the same number of nodes. For example, the 384 (768) GPUs correspond to 96 (192) nodes, which have 3072 (6144) CPU cores. Therefore, the overall speedup is approximately 6.375 (0.51/0.08) for 384 GPUs and 4.15 (0.83/0.2) for 768 GPUs (Figure 10). The speedups are comparable with our previous work porting LICOM2 to GPU using OpenACC (Jiang et al., 2019), which is approximately 1.8-4.6 times the speedup using one GPU card vs. two

Deleted: require
Deleted: much time
Formatted ... [29]
Formatted ... [30]
Deleted: …year simulation, 5-10 SYPD is better. The NCEP ... [31]
Deleted: While…hen the scale increases to 9216 GPUs, the I ... [32]
Formatted ... [33]
Deleted: points
Deleted: line
Formatted ... [34]
Deleted: 100km
Formatted ... [35]
Deleted: grey
Formatted ... [36]
Deleted: line is
Formatted ... [37]
Formatted ... [38]
Deleted: threads
Formatted ... [39]
Deleted: the
Formatted ... [40]
Deleted: grey
Formatted ... [41]
Deleted: the
Formatted ... [42]
Deleted: averagely
Formatted ... [43]
Deleted: whole
Formatted ... [44]
Deleted: operations
Deleted: a little
Formatted ... [45]
Formatted ... [46]
Deleted: stray
Formatted ... [47]
Deleted: whole
Formatted ... [48]
Deleted:
Formatted ... [49]
Deleted: a lot of
Formatted ... [50]
Deleted: times…ime speedup than that of the same number o ... [51]
Deleted: totally
Deleted: about…pproximately 6.375 (0.51/0.08) for 384 GPU ... [52]

8-core Intel GPU in small-scale experiments for specific kernels. Our results are also slightly better than Xu et al. (2015), who ported another ocean model to GPUs using Cuda C. However, due to the limitation of the number of intel CPUs (maximal 9216 cores), we did not obtain the overall speedup for 1536 and more GPUs.

Figure 11 depicts the actual times and speedups of different GPU computations. The green line in Figure 11a is a function of the stepon time cost; it decreases while the GPU number increases. The blue curve of Figure 11a shows the increase in speedup with the rise in the GPU scale. Despite the speedup increase, the efficiency of the model decreases. At 9216 GPUs, the model efficiency starts under 20%, and for more GPUs (19600 and 26200), the efficiency is flattened to approximately 10%. The efficiency decrease is mainly caused by the latency of the data copy in and out to the GPU memory. For economic consideration, the 384-1536 scale is a better choice for realistic modeling studies.

Figure 12 depicts the time cost of seven core subroutines of LICOM3-HIP. We find that the top four most time cost subroutines are "barotr," "tracer," "bclinc," and "readyc", and the other subroutines cost only approximately 1% of the whole computation time. When 384 GPUs are applied, the "barotr" costs approximately 50% of the total time (Figure 12a), which solves the barotropic equations. When GPUs are increased to 9216, each subroutine's time cost decreases, but the percentage of subroutine "barotr" is increased to 62% (Figure 12b). As mentioned above, this phenomenon can be interpreted by having more haloing in "barotr" than in the other subroutines; hence, the memory data copy and communication latency make it slower.

4.2. Model performance in climate research

The daily mean sea surface height (SSH) fields of the CPU and HIP simulations are compared to test the usefulness of the HIP version of LICOM for the numerical precision of scientific usage. Here, the results from 1/20° experiments on a particular day, March 1st of the 4th model year, are used (Figures 13a, b). The general SSH spatial patterns of the two are visually very similar. Significant differences are only found in very limited areas, such as in the eddy-rich regions near strong currents or high-latitude regions (Figure 13c); in most places, the difference in values fall into the range of -0.1 and 0.1 cm. Because the hardware is different and the HIP codes' mathematical operation sequence is not always the same as that for the Fortran version, the HIP and CPU versions are not identical byte-by-byte. Therefore, it is hard to verify the correctness of the results from the HIP version. Usually, the ensemble method is employed to evaluate the consistency of two model runs (Baker et al., 2015). Considering the unacceptable computing and storage resources, in addition to the differences between the two versions, we simply compute root mean square errors (RMSEs) between the two versions, which are only 0.18 cm, much smaller than the spatial variation of the system, which is 92 cm (approximately 0.2%). This indicates that the results of LICO3-HIP are generally acceptable for research.

The GPU version's sea surface temperature (SST) is compared with the observed SST to evaluate the global 1/20° simulation's preliminary results from LICOM3-HIP (Figure 14). Because the LICOM3-HIP experiments are forced by the daily mean atmospheric variables in 2016, we also compare the outputs with the observation data in 2016. Here, the 1/4° Optimum Interpolation Sea Surface Temperature (OISST) is employed for comparison, and the simulated SST is interpolated to the same resolution as the OISST. We find that the global mean values of SST are close together, but with a slight warming bias of

Deleted: which has
Deleted: GPU
Deleted: But
Deleted: didn't
Deleted: GPUs computation.
Deleted: the
Deleted: of
Deleted: of
Deleted: %;
Deleted: about
Deleted: decreasing
Deleted: economical
Deleted: ;
Deleted: about
Deleted: about
Deleted: the
Deleted: being more
Deleted: versions'
Deleted: the
Deleted: visually. The significant
Deleted:
Deleted: besides
Deleted: here
Deleted: Root Mean Square Errors
Deleted: is
Deleted: about
Deleted: That
Deleted: of
Deleted: 's
Deleted: to each other
Deleted: ,

18.49°C for observations vs. 18.96°C for the model. The spatial pattern of SST in 2016 is well reproduced by LICOM3-HIP. The spatial standard deviation (STD) of SST is 11.55°C for OISST and 10.98°C for LICOM3-HIP. The RMSE of LICOM3-HIP against the observation is only 0.84°C.

With an increasing horizontal resolution of the observations, we now know that mesoscale eddies are ubiquitous in the ocean at the 100-300 km spatial scale. Rigorous eddies usually occur along significant ocean currents, such as the Kuroshio and its extension, the Gulf Stream, and the Antarctic Circumpolar Current (Figure 15a). Eddies also capture more than 80% of the ocean's kinetic energy, which was estimated using satellite data (e.g., Chelton et al., 2011). Therefore, these mesoscale eddies must be solved in the ocean model. A numerical model's horizontal resolution must be higher than 1/10° to resolve the global ocean eddies but cannot resolve the eddies in high latitude and shallow waters (Hallberg, 2013). Therefore, a higher resolution is required to determine the eddies globally. The EKE for the 1° version is low, even in the areas with strong currents, while the 1/10° version can reproduce most of the eddy-rich regions in the observation. The EKE increases when the resolution is further enhanced to 1/20°, indicating that many more eddy activities are resolved.

5 Discussion

5.1. Application of the ocean climate model beyond 10000 GPUs

Table 4 summarizes the detailed features of some published GPU version models. We find that various programming methods have been implemented for different models. A near-kilometer atmospheric model using 4888 GPUs was reported as a large-scale example of weather/climate studies. With supercomputing development, the horizontal resolution of ocean circulation models will keep increasing, and more sophisticated physical processes will also be developed. The LICOM3-HIP has a larger scale, not only in terms of grid size but also in final GPU numbers.

We successfully performed a quasi-whole machine (26200 GPUs) test, and the results indicate that the model obtained an increasing SYPD (2.72). The application of an ocean climate model beyond 10000 GPUs is not easy because the multinodes plus multi-GPUs running requires that the network connection, PCI-e and memory speed, and input/output storage systems all work in their best performances. Gupta et al. (2017) investigated 23 types of system failures to improve reliability of the HPC system. Unlike Gupta's study, only the three most common types of failures we encountered are discussed here. The three most common errors when running LICOM3-HIP are MPI hardware errors, CPU memory access errors, and GPU hardware errors. Let us suppose that the probability of an individual hardware (or software) error occurring is 10^{-5} (which means 1 failure in 100000 hours). As the MPI (GPU) scale increases, the total error rate increases, and once a hardware error occurs, the model simulation will fail.

When 384 GPUs are applied, the success rate within one hour can be expressed as $\left(1-384\times10^{-5}\right)^{3}=98.85\%$, and the failure rate is then $1-\left(1-384\times10^{-5}\right)^{3}=1.15\%$. Applying this formula, we can obtain the failure rate corresponding to 1000, 10000, and 26200 GPUs. The results are listed in Table 5. As shown in Table 5, on the medium scale (i.e., 1000 GPUs are used), three

Deleted: Standard Deviation (STDs
Deleted: observation
Deleted: with a
Deleted: The rigorous
Deleted: Extension
Deleted: The eddies
Deleted: ocean's
Deleted: ,
Deleted: that
Deleted: the
Deleted: is increased
Deleted: much
Deleted: can
Deleted: programing
Deleted: multi-nodes
Deleted: Gupta (
Deleted: .,
Deleted: have
Deleted: the
Deleted: HPC systems'
Deleted: .
Deleted: have mostly met
Deleted: occur
Deleted: 's
Deleted: to occur
Deleted: Along with
Deleted: GPUs
Deleted: increasing
Deleted: is increased;
Deleted:
Deleted: in
Deleted: -

failures will occur through 100 runs; when the scale increases to 10000 GPUs, 1/4 of them will fail. The 10^{-5} error probability also indicates that 10000 GPU tasks cannot run ten continuous hours on average. If the success time restriction decreases, the model success rate will increase. For example, within 6 minutes, the 26200 GPU task success rate is $\left(1\text{-}26200\times10^{-6}\right)^{3}$=92.34%, and its failure rate is 1-$\left(1\text{-}26200\times10^{-6}\right)^{3}$=7.66%.

5.2. Energy to solution

We also measured energy to solution here. A simulation normalized energy (E) is employed here as a metric. The formula is as follows:

$$E = TDP \times N \times 24/SYPD$$

where TDP is the thermal design power, N is the computer nodes used, and SYPD/24 equals the simulated years per hour. Therefore, the smaller the E value is, the better, which means that we can obtain more simulated years within a limited power supply. To calculate E's value, we estimated the TDP of 1380 W for a node on the present platform (1 AMD CPU and 4 GPUs) and 290 W for a reference node (2 Intel 16-core CPUs). We only include the TDP of CPUs and GPUs here.

Based on the above power measurements, simulations' energy cost is shown in Table 6 in MWh per simulation year (MWh/SY). The energy costs for the 1/20° LICOM3 simulations running on CPUs and GPUs are comparable when the numbers of MPI processors are within 1000. The energy costs of LICOM3 at 1/20° running on 384 (768) GPUs and CPUs are approximately 6.234 (7.661) MWh/SY and 6.845 (6.280) MWh/SY, respectively. However, the simulation speed of LICOM3 on a GPU is much faster than that on a CPU, approximately 42 times for 384 processors and 31 times for 768 processors. When the number of MPI processors is beyond 1000, the value of E for the GPU becomes much larger than that for the CPU. This result indicates that the GPU is not fully loaded at this scale.

6 Conclusion

The GPU version of LICOM3 under the HIP framework was developed in the present study. Seven kernels within the time integration of the mode are all ported to the GPU, and 3-D parallelization (also partitioned in the vertical direction) is applied. The new model was implemented and gained an excellent acceleration rate on a Linux cluster with AMD GPU cards. This is also the first time an ocean general circulation model has been fully applied on a heterogeneous supercomputer using the HIP framework. It totally took nineteen months, five Ph.D. students and five part-time staff to finish the porting and testing work. Based on our test using the 1/20° configuration, LICOM3-HIP is 42 times faster than the CPU when 384 AMD GPUs and CPU cores are used. LICOM3-HIP has good scalability, and can obtain a speedup of more than four on 9216 GPUs compared to 384 GPUs. The SYPD, which is in equilibrium with the speedup, continues to increase as the number of GPUs increases. We successfully performed a quasi-whole machine test, which was 6550 nodes and 26200 GPUs, using 1/20° LICOM3-HIP on the supercomputer, and at the grand scale, the model can obtain an increasing SYPD of 2.72. The modification or

Deleted: happen
Deleted: GPUs task
Deleted: GPUs
Deleted: has been
Deleted: Thermal Design Power
Deleted: So
Deleted: get
Deleted: Simulation Year
Deleted: about
Deleted: But
Deleted: about
Deleted: from
Deleted: **Conclusions**
Deleted: has been
Deleted: The dynamic core and physic packages
Deleted: both
Deleted: has been
Deleted: accelerating
Formatted: Font color: Text 1
Deleted: is
Formatted: Font color: Text 1
Deleted: and
Formatted: Font color: Text 1
Deleted: the
Formatted: Font color: Text 1
Deleted: fast
Formatted: Font color: Text 1
Deleted: does,
Formatted: Font color: Text 1
Deleted: The
Deleted: it
Deleted: still
Deleted: comparing
Deleted: to
Deleted: keeps increasing
Deleted: still

optimization of the model also improves the 10- and 100-km performances, although we did not analyze their performances in this article.

The efficiency of the model decreases with the increasing number of GPUs. At 9216 GPUs, the model efficiency starts under 20% against 384 GPUs, and when the number of GPUs reaches or exceeds 20000, the efficiency is only approximately 10%. Based on our kernel functions test, the decreasing efficiency was mainly caused by the latency of data copy in and out to the GPU memory in solving the barotropic equations, particularly for the number of GPUs larger than 10000.

Using the 1/20° configuration of LICOM3-HIP, we conducted a 14-year spin-up integration. Because the hardware is different and the GPU codes' mathematical operation sequence is not always the same as that of the Fortran version, the GPU and CPU versions cannot be identical byte by byte. The comparison between the GPU and CPU versions of LICOM3 shows that the differences in most places are minimal, indicating that the results from LICOM3-HIP can be used for practical research. Further comparison with the observation and the lower-resolution results suggests that the 1/20° configuration of LICOM3-HIP can reproduce the observed large-scale features and produce much smaller-scale activities than that of lower-resolution results. The eddy-resolving ocean circulation model, which is a virtual platform for oceanography research, ocean forecasting, and climate prediction and projection, can simulate the variations in circulations, temperature, salinity, and sea level with a spatial scale larger than 15 km and temporal scale from the diurnal cycle to decadal variability. As mentioned above, 1-2 SYPD is a good entrance for a realistic climate research model. The more practical GPU scale range for realistic simulation is approximately 384-1536 GPUs. At these scales, the model still has 0.5-1.22 SYPD. Even if we decrease the loops in the "barotr" procedure to 1/3 of the original in the spin-up simulation, the performance will achieve 1-2.5 SYPD for 384-1536 GPUs. This performance will satisfy 10-50-year scale climate studies. In addition, this version can be used for short-term ocean prediction in the future.

Additionally, the block size of 36×30×55 (1/20° setup, 26200 GPUs) is not an enormous computational task for one GPU. Since one GPU has 64 cores total of 2560 threads, if a subroutine computation is 2-D, each thread's operation is too small. Even for the 3-D loops, it is still not large enough to load the entire GPU. This indicates that it will gain more speedup when the LICOM resolution is increased to the kilometer level. The LICOM3-HIP codes are now written for 1/20°, but they are kilometer-ready GPU codes.

The optimization strategies here are mostly at the program level and do not treat the dynamic or physics parts separately. We only ported all seven core subroutines within the time integration loops to the GPU, including both the dynamic and physics parts. Unlike atmospheric models, there are few time-consuming physical processes in ocean models, such as radiative transportation, clouds, precipitation, and convection processes. Therefore, the two kinds of parts are usually not separated in the ocean model, particularly in the early stage of model development. This is also the case for LICOM. Further optimization to explicitly separate the dynamic core and the physical package is necessary in the future.

There is still potential to further increase the speedup of LICOM3-HIP. The bottleneck is in the high-frequency data copy in and out to the GPU memory in the barotropic part of the LICOM3. Unless HIP-aware MPI is supported, the data transfer latency between the CPU and GPU cannot be overcome. Thus far, we can only reduce the time consumed by decreasing the

Deleted:
Deleted:
Deleted: ;
Deleted: about
Deleted: have
Deleted: more
Deleted: forecast
Deleted: of the
Deleted: around
Deleted: Besides
Deleted: Besides
Deleted: computation
Deleted: big
Deleted: whole
Deleted: optimizing
Deleted: ,
Deleted: the
Deleted: no many
Deleted: the
Deleted: model
Deleted: the
Deleted: cloud
Deleted: particular
Deleted: of
Deleted: should be done
Deleted:
Deleted: the
Deleted: So

frequency or magnitude of the data copy and even modifying the method to solve the barotropic equations. Additionally, using single precision within the time integration of LICOM3 might be another solution. The mixing precision method has already been tested using an atmospheric model, and the average gain in computational efficiency is approximately 40% (Váňa et al., 2017). We would like to try these methods in the future.

Deleted: the
Deleted: -
Deleted: an
Deleted: by

Code availability

The model code (LICOM3-HIP V1.0) along with the dataset and a 100 km case can be downloaded from the website https://zenodo.org/record/4302813#.X8 mGWcsvNb8 with the Digital Object Identifier (doi): 10.5281/zenodo.4302813.

Deleted: 100km
Deleted: X8mGWcsvNb8

Data availability

The data for figures in this paper can be downloaded from https://zenodo.org/record/4542544#._YCs24c8vPII with doi: 10.5281/zenodo.4542544.

Author contribution

Pengfei Wang: Software, visualization, formal analysis, and writing-original draft

Deleted: Visualization, Formal

Jinrong Jiang: Software and Writing – review & editing
Pengfei Lin: Software and Writing – review & editing
Mengrong Ding: Visualization and Data curation
Junlin Wei: Software
Zhang Feng: Software
Lian Zhao: Software
Yiwen Li: Software and Visualization
Zipeng Yu: Software and Data curation
Weipeng Zheng: Formal analysis
Yongqiang Yu: Conceptualization
Xuebin Chi: Conceptualization
Hailong Liu: Supervision, Formal analysis, and writing-original draft

Competing interests:

The authors declare that they have no known competing financial interests or personal relationships that could have appeared to influence the work reported in this paper.

Acknowledgments

The study is funded by the National Natural Sciences Foundation (41931183), the National Key Research and Development Program (2018YFA0605904 and 2018YFA0605703), and the Strategic Priority Research Program of the Chinese Academy of Sciences (XDC01040100). Dr.s H.L.L. and P.F.L. were also supported by the "Earth System Science Numerical Simulator Facility" (EarthLab).

Deleted:

References

Baker, A. H., Hammerling, D. M., Levy, M. N., Xu, H., Dennis, J. M., Eaton, B. E., Edwards, J., Hannay, C., Mickelson, S. A., Neale, R. B., Nychka, D., Shollenberger, J., Tribbia, J., Vertenstein, M., and Williamson, D.: A new ensemble-based consistency test for the Community Earth System Model (pyCECT v1. 0), *Geosci. Model Dev.*, 8, 2829-2840, https://doi.org/10.5194/gmd-8-2829-2015, 2015.

Balaji, V., Maisonnave, E., Zadeh, N., Lawrence, B. N., Biercamp, J., Fladrich, U., Aloisio, G., Benson, R., Caubel, A., Durachta, J., Foujols, M.-A., Lister, G., Mocavero, S., Underwood, S., and Wright, G.: CPMIP: measurements of real computational performance of Earth system models in CMIP6, *Geosci. Model Dev.*, 10, 19–34, https://doi.org/10.5194/gmd-10-19-2017, 2017.

Canuto, V., Howard, A., Cheng, Y., and Dubovikov, M.: Ocean turbulence. Part I: One-point closure model—Momentum and heat vertical diffusivities, *J. Phys. Oceanogr.*, 31, 1413-1426, https://doi.org/10.1175/1520-0485(2001)031<1413:OTPIOP>2.0.CO;2, 2001.

Canuto, V., Howard, A., Cheng, Y., and Dubovikov M.: Ocean turbulence, Part II: Vertical diffusivities of momentum, heat, salt, mass, and passive scalars, *J. Phys. Oceanogr.*, 32(1), 240-264, https://doi.org/10.1175/1520-0485(2002)032<0240:OTPIVD>2.0.CO;2, 2002.

Chassignet, E. P., Sommer, J. L., and Wallcraft A. J: General Circulation Models In "Encyclopedia of Ocean Sciences (3rd edition)", Cochran, K. J., Bokuniewicz, H. J., and Yager P. L. (Eds.), 5, 486-490, https://doi.org/10.1016/B978-0-12-409548-9.11410-1, 2019.

Chassignet, E. P., Yeager, S. G., Fox-Kemper, B., Bozec, A., Castruccio, F., Danabasoglu, G., Kim, W. M., Koldunov, N., Li, Y., Lin, P., Liu, H., Sein, D. V., Sidorenko, D., Wang, Q., and Xu, X.: Impact of horizontal resolution on global ocean-sea-ice model simulations based on the experimental protocols of the Ocean Model Intercomparison Project phase 2 (OMIP-2), *Geosci. Model Dev.*, 1-58, https://doi.org/10.5194/gmd-2019-374, 2020.

Chelton, D. B., Schlax, M. G., & Samelson R. M.: Global observations of nonlinear mesoscale eddies, *Prog. Oceanogr.*, 91(2), 167-216, https://doi.org/10.1016/j.pocean.2011.01.002, 2011.

Craig, A. P., Vertenstein, M. and Jacob, R.: A new flexible coupler for earth system modeling developed for CCSM4 and CESM1, *The International Journal of High Performance Computing Applications*, 26(1), 31-42, https://doi.org/10.1177/1094342011428141, 2012.

Ferreira, D., Marshall, J. and Heimbach, P.: Estimating eddy stresses by fitting dynamics to observations using a residual-mean ocean circulation model and its adjoint, *J. Phys. Oceanogr.*, 35(10), 1891-1910, https://doi.org/10.1175/JPO2785.1, 2005.

Fox-Kemper, B., and Menemenlis D.: Can Large Eddy Simulation Techniques Improve Mesoscale-Rich Ocean Models? In: Ocean Modeling in an Eddying Regime, edited by: Hecht, M.W., and Hasumi H., 177, 319-338, https://doi.org/10.1029/177GM19, 2008.

Fuhrer, O., Chadha, T., Hoefler, T., Kwasniewski, G., Lapillonne, X., Leutwyler, D., Lüthi, D., Osuna, C., C., Schär, C., Schulthess, T. C., and Vogt, H., Near-global climate simulation at 1 km resolution: establishing a performance baseline on 4888 GPUs with COSMO 5.0, *Geosci. Model Dev.*, 11(4), 1665-1681, https://doi.org/10.5194/gmd-11-1665-2018, 2018.

Gent, P. R., and J. C. Mcwilliams: Isopycnal mixing in ocean circulation models, *J. Phys. Oceanogr.*, 20(1), 150-155, https://doi.org/10.1175/1520-0485(1990)020<0150:IMIOCM>2.0.CO;2, 1990.

Griffies, S. M., Winton, M., Anderson, W. G., Benson, R., Delworth, T. L., Dufour, C. O., Dunne, J. P., Goddard, P., Morrison, A. K., Rosati, A., Wittenberg, A. T., Yin, J., and Zhang, R.: Impacts on ocean heat from transient mesoscale eddies in a hierarchy of climate models, *J. Climate*, 28(3), 952-977, https://doi.org/10.1175/JCLI-D-14-00353.1, 2015.

Griffies, S., Danabasoglu, G., Durack, P., Adcroft, A., Balaji, V., Böning, C., Chassignet, E., Curchitser, E., Deshayes, J., Drange, H., Fox-Kemper, B., Gleckler, P. J., Gregory, J. M., Haak, H., Hallberg, R. W., Heimbach, P., Hewitt, H. T., Holland, D. M., Ilyina, T., Jungclaus, J. H., Komuro, Y., Krasting, J. P., Large, W. G., Marsland, S. J., Masina, S., McDougall, T. J., Nurser, A. J. G., Orr, J. C., Pirani, A., Qiao, F., Stouffer, R. J., Taylor, K. E., Treguier, A. M., Tsujino, H., Uotila, P., Valdivieso, M., Wang, Q., Winton, M., and Yeager, S. G.: OMIP contribution to CMIP6: experimental and diagnostic protocol for the physical component of the Ocean Model Intercomparison Project, *Geosci. Model Dev.*, 9(9), https://dx.doi.org/10.5194/gmd-9-3231-2016, 2016.

Gupta, S., Patel, T., Engelmann, C., and Tiwari, D.: Failures in Large Scale Systems: Long-term Measurement, Analysis, and Implications. In *Proceedings of SC17*, Denver, CO, USA, November 12-17, https://dx.doi.org/10.1145/3126908.3126937, 2017.

Hallberg, R.: Using a resolution function to regulate parameterizations of oceanic mesoscale eddy effects, *Ocean Model.*, 72, 92-103, https://dx.doi.org/10.1016/j.ocemod.2013.08.007, 2013.

He, B., Yu, Y., Bao, Q., Lin, P. F., Liu, H. L., Li, J. X., Wang, L., Liu, Y. M., Wu, G., Chen, K., Guo, Y. Zhao, S., Zhang, X., Song, M., and Xie, J.: CAS FGOALS-f3-L model dataset descriptions for CMIP6 DECK experiments, *Atmos. Oceanic Sci. Lett.*, 1-7, https://dx.doi.org/10.10801/16742834.2020.1778419, 2020.

Hewitt, H. T., Bell, M. J., Chassignet, E. P., Czaja, A., Ferreira, D., Griffies, S. M., Hyder, P., McClean, J. L., New, A.L., and Roberts, H. J.: Will high-resolution global ocean models benefit coupled predictions on short-range to climate timescales? *Ocean Model.*, 120, 120-136, https://dx.doi.org/10.1016/j.ocemod.2017.11.002, 2017.

Jiang, J., Lin, P., Wang, J., Liu, H., Chi, X., Hao, H., Wang, Y., Wang, W., and Zhang, L. H.: Porting LASG/IAP Climate System Ocean Model to GPUs Using OpenAcc, *IEEE Access*, 7, 154490-154501, https://dx.doi.org/10.1109/ACCESS.2019.2932443, 2019.

Large, W. G., and Yeager, S. G.: The global climatology of an interannually varying air-sea flux data set, *Clim. Dyn.*, 33, 341−364, https://doi.org/10.1007/s00382-008-0441-3, 2009.

Li, L., Yu, Y., Tang, Y., Lin, P., Xie, J., Song, M., Dong, L., Zhou, T., Liu, L., Wang, L., Pu, Y., Chen, X. L., Chen, L., Xie, Z. H., Liu, H. B., Zhang, L. X., Huang, X., Feng, T., Zheng, W. P., Xia, K., Liu, H. L., Liu, J. P., Wang, Y., Wang, L. H., Jia, B. H., Xie, F., Wang, B., Zhao, S. W., Yu, Z. P., Zhao, B. W., and Wei, J. L.: The Flexible Global Ocean Atmosphere Land System Model Grid Point Version 3 (FGOALS-g3): Description and Evaluation, *J. Adv. Model Earth Sy.*, https://dx.doi.org/10.1029/2019MS002012, 2020.

Li, Y. W., Liu, H. L., Ding, M. R., Lin, P. F., Yu, Z. P., Meng, Y., Li, Y. L., Jian, X. D., Jiang, J. R., Chen, K. J., Yang, Q., Wang, Y. Q., Zhao, B. W., Wei, J. L., Ma, J. F., Zheng, W. P., and Wang, P. F.: Eddy-resolving Simulation of CAS-LICOM3 for Phase 2 of the Ocean Model Intercomparison Project, *Adv. Atmos. Sci.*, 37(10), 1067-1080, https://doi.org/ 10.1007/s00376-020-0057-z., 2020.

Lin, P., Liu, H., Xue, W., Li, H., Jiang, J., Song, M., Song, Y., Wang, F., and Zhang, M. H.: A Coupled Experiment with LICOM2 as the Ocean Component of CESM1, *J. Meteorol. Res.*, 30(1), 76-92, https://dx.doi.org/10.1007/s13351-015-5045-3, 2016.

Lin, P., Yu, Z., Liu, H., Yu, Y., Li, Y., Jiang, J., Xue, W., Chen, K., Yang, Q., Zhao, B. W., Wei, J. L., Ding, M. R., Sun, Z. K., Wang, Y. Q., Meng, Y., Zheng, W. P., and Ma, J. F.: LICOM Model Datasets for the CMIP6 Ocean Model Intercomparison Project, *Adv. Atmos. Sci.*, 37(3), 239-249, https://dx.doi.org/10.1007/s00376-019-9208-5, 2020.

Liu, H., Lin, P., Yu, Y., and Zhang X.: The baseline evaluation of LASG/IAP climate system ocean model (LICOM) version 2, *Acta Meteorol. Sin.*, 26(3), 318-329, https://doi.org/10.1007/s13351-012-0305-y, 2012.

Liu, H. L., Lin, P., Zheng, W., Luan, Y., Ma, J., Mo, H., Wan L., and Tiejun Ling: A global eddy-resolving ocean forecast system – LICOM Forecast System (LFS), *J. Oper. Oceanogr.*, DOI:10.1080/1755876X.2021.1902680.

Madec, G., and Imbard, M.: A global ocean mesh to overcome the North Pole singularity, *Clim. Dyn.*, 12(6), 381-388, https://doi.org/10.1007/s003820050115, 1996.

Murray, R. J.: Explicit generation of orthogonal grids for ocean models, *J. Comput. Phys.*, 126(2), 251-273, https://doi.org/10.1006/jcph.1996.0136, 1996.

Ohlmann, J. C.: Ocean radiant heating in climate models, *J. Climate*, 16(9), 1337-1351, https://doi.org/10.1175/1520-0442-16.9.1337, 2003

Deleted: under review, 2020

Palmer, T.: Climate forecasting: Build high-resolution global climate models, *Nature News*, 515(7527), 338-339, https://doi.org/10.1038/515338a, 2014.

Redi, M. H.: Oceanic isopycnal mixing by coordinate rotation, *J. Phys. Oceanogr.*, 12(10), 1154-1158, https://doi.org/10.1175/1520-0485(1982)012<1154:OIMBCR>2.0.CO;2, 1982.

Schär, C., Fuhrer, O., Arteaga, A., Ban, N., Charpilloz, C., Di Girolamo, S., Hentgen, L., Hoefler, T., Lapillonne, X., Leutwyler, D., Osterried, K., Panosetti, D., Rüdisühli, S., Schlemmer, L., Schulthess, T. C., Sprenger, M., Ubbiali, S., and Wernli, H.: Kilometer-scale climate models: Prospects and challenges, *Bull. Am. Meteorol. Soc.*, 101(5), E567-E587, https://doi.org/10.1175/BAMS-D-18-0167.1, 2020.

St. Laurent, L., Simmons, H., and Jayne, S.: Estimating tidally driven mixing in the deep ocean, *Geophys. Res. Lett.*, 29(23), https://doi.org/ 10.1029/2002GL015633, 2002.

Su, Z., Wang, J., Klein, P., Thompson, A. F., and Menemenlis, D.: Ocean submesoscales as a key component of the global heat budget, *Nature communications*, 9(1), 1-8, https://doi.org/ 10.1038/s41467-018-02983-w, 2018.

Tsujino, H., Urakawa, S., Nakano, H., Small, R., Kim, W., Yeager, S., Danabasoglu, G., Suzuki, T., Bamber, J. L., Bentsen, M., Böning, C. W., Bozec, A., Chassignet, E. P., Curchitser, E., Dias, F. B., Durack, P. J., Griffies, S. M., Harada, Y., Ilicak, M., Josey, S. A., Kobayashi, C., Kobayashi, S., Komuro, Y., Large, W. G., Le Sommer, J., Marsland, S. J., Masina, S., Scheinert, M., Tomita, H., Valdivieso, M., Yamazaki, D.: JRA-55 based surface dataset for driving ocean - sea-ice models (JRA55-do), *Ocean Model.*, 130, 79-139, https://dx.doi.org/10.1016/j.ocemod.2018.07.002, 2018.

Tsujino, H., Urakawa, L. S., Griffies, S. M., Danabasoglu, G., Adcroft, A. J., Amaral, A. E., Arsouze, T., Bentsen, M., Bernardello, R., Böning, C., Bozec, A., Chassignet, E., Danilov, S., Dussin, R., Exarchou, E., Fogli, P., Fox-Kemper, B., Guo, C., Ilicak, M., Iovino, D., Kim, W., Koldunov, N., Lapin, V., Li, Y. W., Lin, P. F., Lindsay, K., Liu., H. L., Long, M., Komuro, Y., Marsland, S., Masina, S., Nummelin, A., Rieck, J., Ruprich-Robert, Y., Scheinert, M., Sicardi, V., Sidorenko, D., Suzuki, T., Tatebe, H., Wang, Q., Yeager, S., and Yu, Z. P.: Evaluation of global ocean–sea-ice model simulations based on the experimental protocols of the Ocean Model Intercomparison Project phase 2 (OMIP-2), *Geosci. Model Dev.*, 13(8), 3643-3708, https://dx.doi.org/10.5194/gmd-13-3643-2020, 2020.

Váňa, F., Düben, P., Lang, S., Palmer, T., Leutbecher, M., Salmond, D., and Carver, G.: Single Precision in Weather Forecasting Models: An Evaluation with the IFS, *Mon. Weather Rev.*, 145(2), 495-502, https://dx.doi.org/10.1175/mwr-d-16-0228.1, 2017.

Wang, S., Jing, Z., Zhang, Q., Chang, P., Chen, Z., Liu, H. and Wu L.: Ocean Eddy Energetics in the Spectral Space as Revealed by High-Resolution General Circulation Models, *J. Phys. Oceanogr.*, 49(11), 2815-2827, https://doi.org/10.1175/JPO-D-19-0034.1, 2019.

Xiao, C.: Adoption of a two-step shape-preserving advection scheme in an OGCM and its coupled experiment, Master thesis, Institute of Atmospheric Physics, Chinese Academy of Sciences, 78pp, 2006.

Xu, S., Huang, X., Oey, L. Y., Xu, F., Fu, H., Zhang, Y., and Yang, G.: POM. gpu-v1. 0: a GPU-based Princeton Ocean Model, *Geosci. Model Dev.*, 8(9), 2815-2827, https://doi.org/10.5194/gmd-8-2815-2015, 2015.

Yang, C., Xue, W., Fu, H., You, H., Wang, X., Ao, Y., Liu, F., Gan, L., Xiu, P., and Wang, L.: 10M-core scalable fully-implicit solver for nonhydrostatic atmospheric dynamics. Paper presented at SC'16: Proceedings of the International Conference for High Performance Computing, Networking, Storage and Analysis, IEEE, 2016.

Yashiro, H., Terai, M., Yoshida, R., Iga, S., Minami, K., and Tomita, H.: Performance analysis and optimization of nonhydrostatic icosahedral atmospheric model (NICAM) on the K computer and TSUBAME2, 5, Paper presented at Proceedings of the Platform for Advanced Scientific Computing Conference, 2016.

Yu, Y., Tang, S., Liu, H., Lin, P., and Li, X.: Development and evaluation of the dynamic framework of an ocean general circulation model with arbitrary orthogonal curvilinear coordinate, *Chinese J. Atmospheric Sci.*, 42(4), 877-889, https://doi.org/1006-9895(2018)42:4<877:RYZJQX>2.0.TX;2-B, 2018.

Yuan, Y., Shi, F., Kirby, J. T., and Yu, F.: FUNWAVE-GPU: Multiple-GPU Acceleration of a Boussinesq-Type Wave Model, *J. Adv. Model Earth Sy.*, 12(5), https://doi.org/ 10.1029/2019MS001957, 2020.

Zhang, X., and Liang, X.: A numerical world ocean general circulation model, *Adv. Atmos. Sci*., 6(1), 44-61, https://doi.org/0256-1530(1989)6:1<44:ANWOGC>2.0.TX;2-S, 1989.

Zhang, H., M., Jin, J., Fei, K., Ji, D., Wu, C., Zhu, J., He, J., Chai, Z. Y., Xie, J. B., Dong, X., Zhang, D. L., Bi, X. Q., Cao, H., Chen, H. S., Chen, K. J., Chen, X. S., Gao, X., Hao, H. Q., Jiang, J. R., Kong, X. H., Li, S. G., Li, Y. C., Lin, P. F., Lin, Z. H., Liu, H. L., Liu, X. H., Shi, Y., Song, M. R., Wang, H. J., Wang, T. Y., Wang, X. C., Wang, Z. F., Wei, Y., Wu, B. D., Xie, Z. H., Xu, Y. F., Yu, Y. Q., Yuan, L., Zeng, Q. C., Zeng, X. D., Zhao, S. W., Zhou, G. Q., and Zhu, J.: CAS-ESM2: Description and Climate Simulation Performance of the Chinese Academy of Sciences (CAS) Earth System Model (ESM) Version 2, *J. Adv. Model Earth Sy.*, 12, e2020MS002210. https://doi.org/10.1029/2020MS002210, 2020.

Shaoqing Zhang, Haohuan Fu, LixinWu, Yuxuan Li, Hong Wang, Yunhui Zeng, Xiaohui Duan,WubingWan, Li Wang, Yuan Zhuang, Hongsong Meng, Kai Xu, Ping Xu, Lin Gan, Zhao Liu,SihaiWu, Yuhu Chen, Haining Yu, Shupeng Shi, Lanning Wang, Shiming Xu, Wei Xue, Weiguo Liu,Qiang Guo, Jie Zhang, Guanghui Zhu, Yang Tu, Jim Edwards, Allison Baker, Jianlin Yong, Man Yuan,Yangyang Yu, Qiuying Zhang, Zedong Liu, Mingkui Li, Dongning Jia, Guangwen Yang, Zhiqiang Wei, Jingshan Pan, Ping Chang, Gokhan Danabasoglu, Stephen Yeager, Nan Rosenbloom, and Ying Guo.: Optimizing high-resolution Community Earth System Model on a heterogeneous many-core supercomputing platform, *Geosci. Model Dev.*, 13, 4809-4829, https://doi.org/10.5194/gmd-13-4809-2020, 2020.

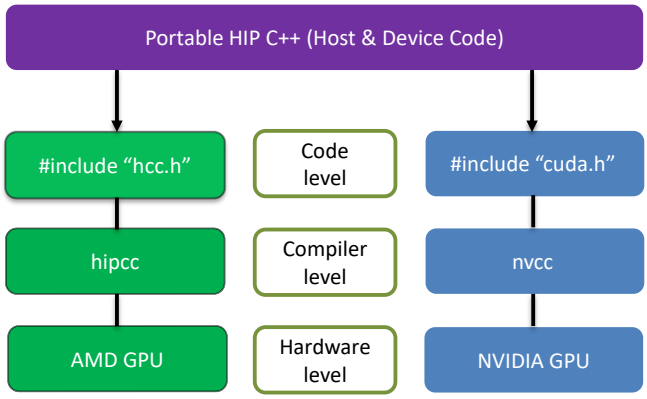

Figure 1: Schematic diagram of the comparison of coding on AMD and NVIDIA GPUs at three levels.

Deleted: The schematic

Deleted: GPU in

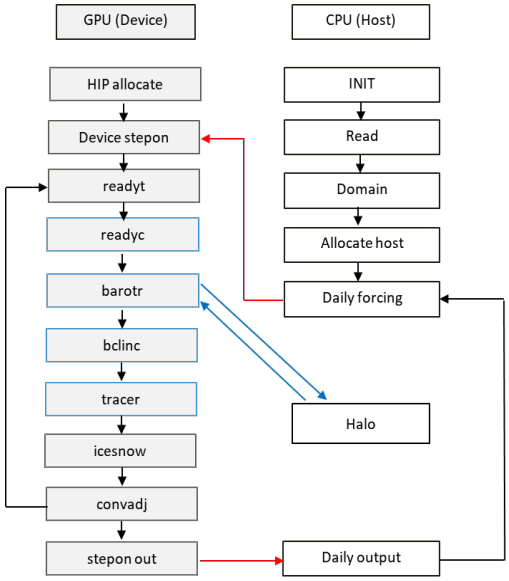

405

Figure 2: LICOM3 computation flowchart with a GPU (HIP device). The red line indicates whole block data transfer between the host and GPU, while the blue line indicates transferring only lateral data of a block.

Deleted: means only

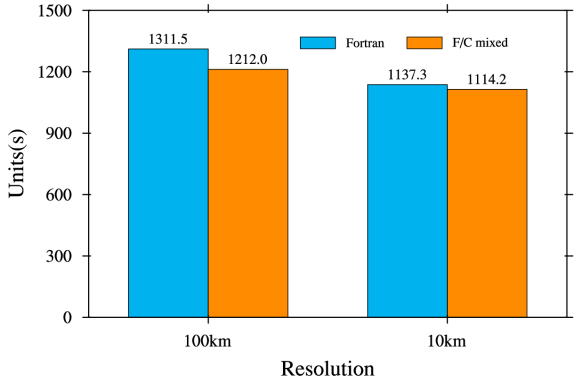

Figure 3: The wall clock time of a model day for the 10 km version and a model month for the 100 km version. The blue and orange bars are for the Fortran and Fortran and C mixed versions. These tests were conducted on an Intel Xeon CPU platform (E5-2697A v4, 2.60 GHz). We used 28 and 280 cores for the low and high resolutions, respectively.

Deleted: 10km
Deleted: 100km
Deleted: the
Deleted: version
Deleted: a platform of
Deleted: 60GHz
Deleted: resolution

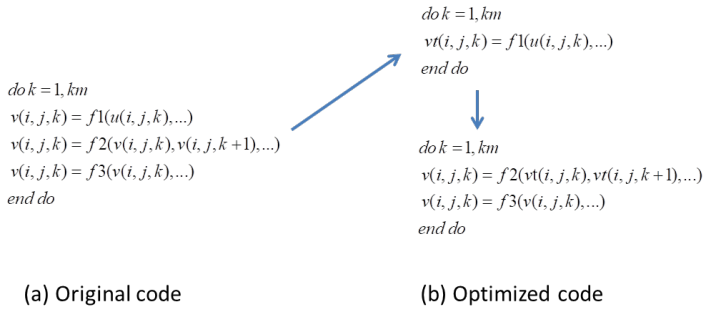

Figure 4: The code using temporary arrays to avoid data dependency.

1425

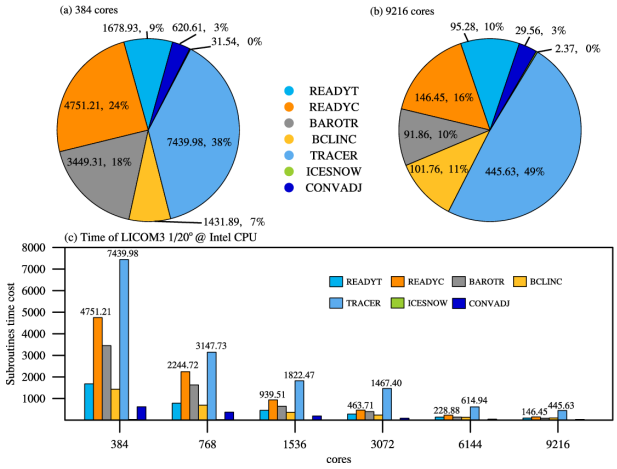

Figure 5: The seven core subroutines' time cost percentages for (a) 384 and (b) 9216 CPU cores. (c) The subroutines' time cost at different scales of LICOM3 (1/20°). These tests were conducted on an Intel Xeon CPU platform (E5-2697A v4, 2.60 GHz).

Deleted: **percentage**

Deleted: **the**

Deleted: **a platform of**

Deleted: **60GHz**

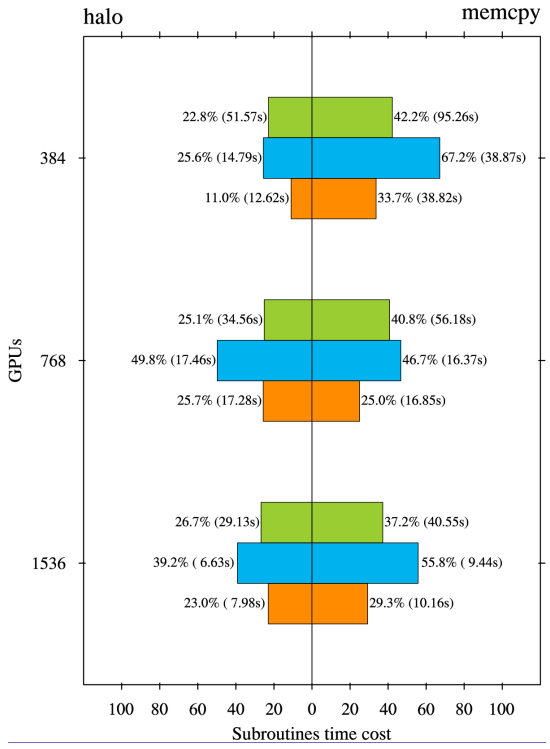

Figure 6: The ratio of the time cost of halo update and memory copy to the total time cost for the three subroutines, "barotr" (green), "bclinc" (blue), and "tracer" (orange), in the HIP version LICOM for three scales (Unit: %). The numbers in the blankets are the time cost of the two processes (unit: second).

Deleted:)

Deleted:

Deleted: Unit

Deleted:

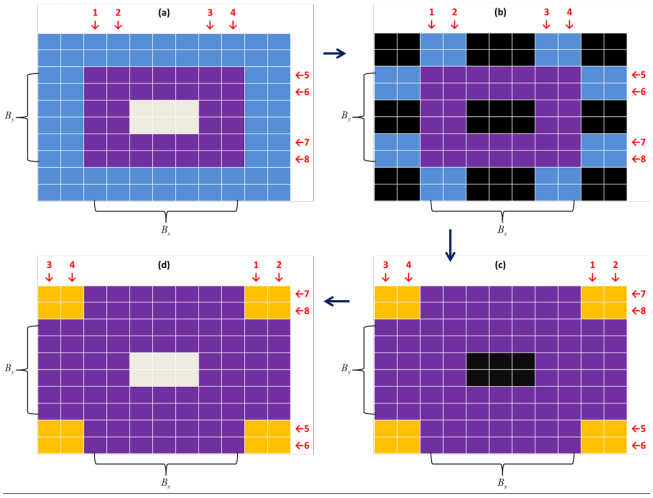

Figure 7: The lateral packing (only transferring four rows and four columns of data between the GPU and CPU) method to accelerate the halo. (a) In the GPU space, where central (gray) grids are unchanged; (b) transferred to the CPU space, where black grids mean no data; (c) after halo with neighbors; and (d) transfer back to the GPU space.

Deleted: transfer

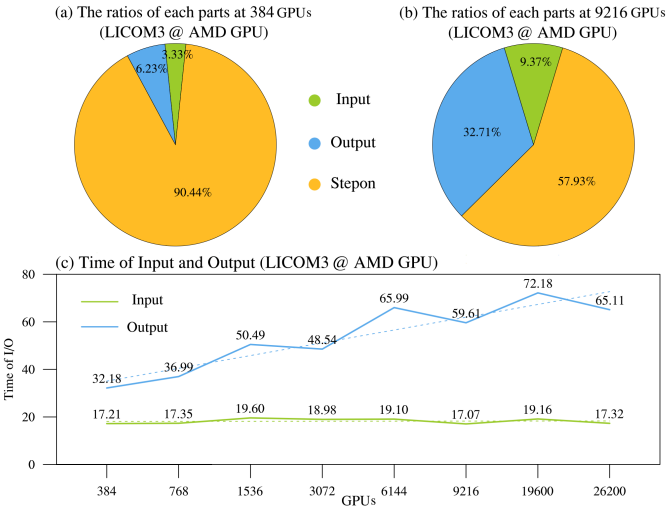

Figure 8: (a) The 384 GPUs, (b) 9216 GPUs, the I/O ratio in total simulation time for 1/20° setup, and (c) the changes of I/O times versus different GPUs.

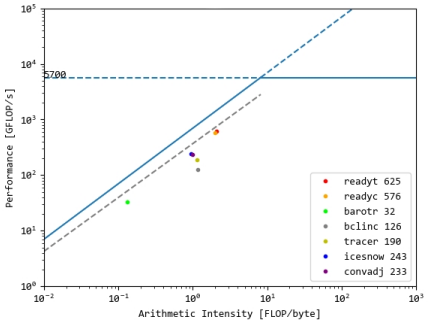

Figure 9: Roofline model for the AMD GPU and the performance of LICOM's main subroutines.

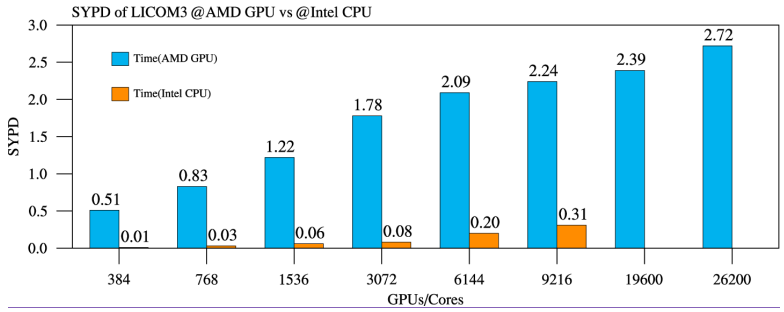

Figure 10: Simulation performances of the AMD GPU versus Intel CPU core for LICOM3 (1/20°). Unit: SYPD.

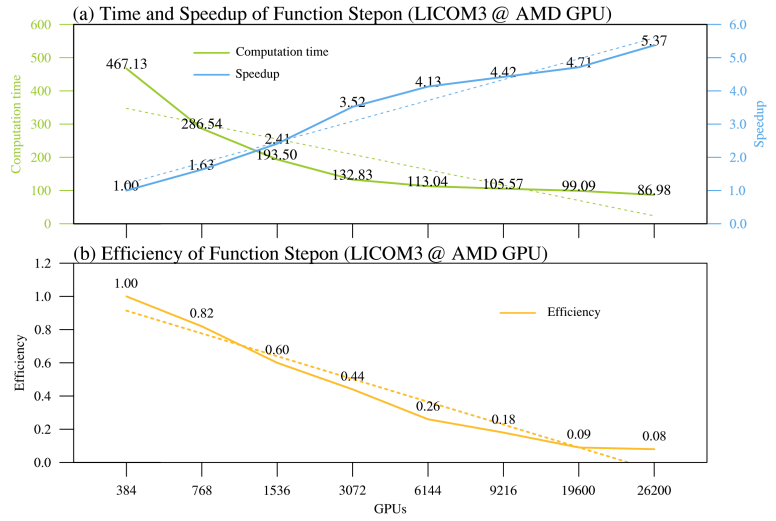

Figure 11: (a) Computation time (green) and speedup (blue) and (b) parallel efficiency (orange) at different scales for stepons of LICOM3-HIP (1/20°).

Deleted:),

Deleted: **stepon**

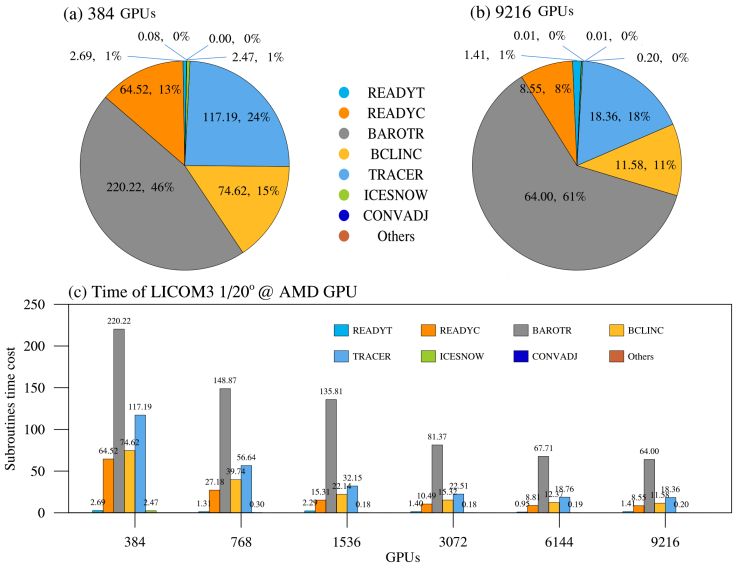

Figure 12: The seven core subroutines' time cost percentages for (a) 384 GPUs and (b) 9216 GPUs. (c) The subroutines' time cost at different scales of LICOM3-HIP (1/20°).

Deleted: **percentage**

Deleted: **The**

Deleted: **the**

1470

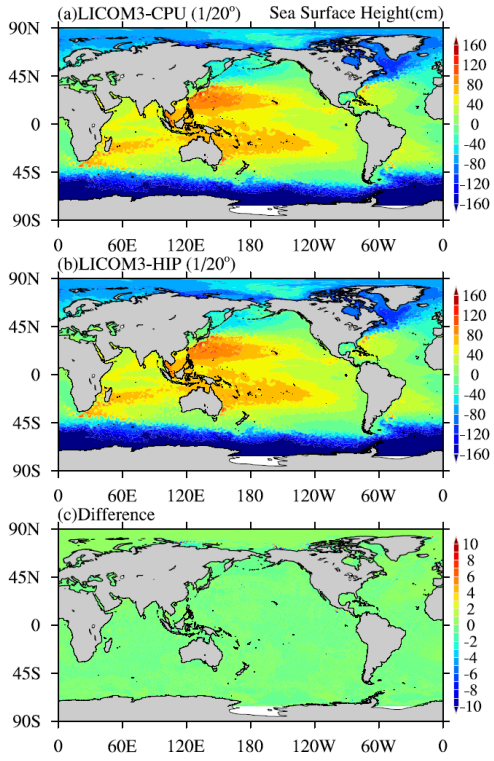

Figure 13: Daily mean simulated sea surface height for (a) CPU and (b) HIP versions of LICOM3 at 1/20° on March 1st of the 4th model year. (c) The difference between the two versions (HIP minus CPU). Units: cm.

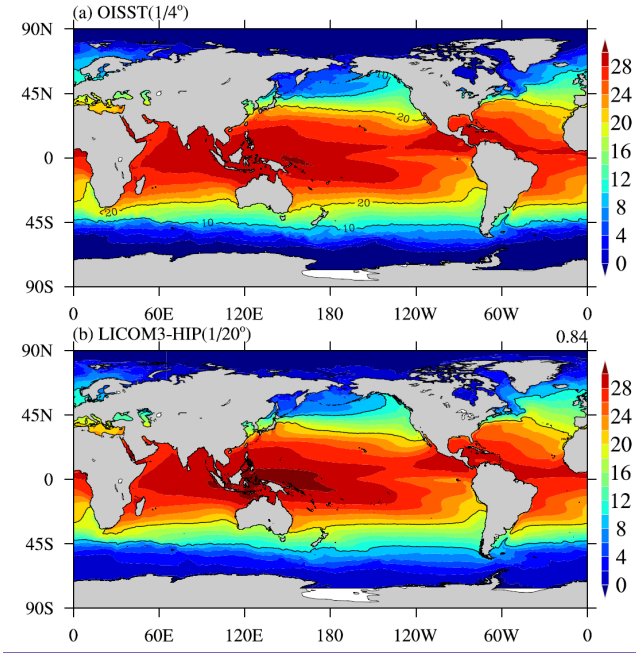

Figure 14: (a) Observed annual mean sea surface temperature in 2016 from the Optimum Interpolation Sea Surface Temperature (OISST); (b) simulated annual mean SST for LICOM3-HIP at 1/20° during model years 0005-0014. Units: °C.

Deleted: the

Deleted: the

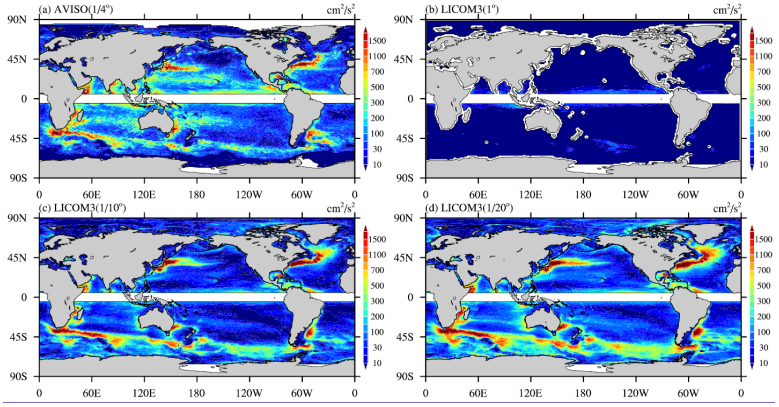

Figure 15: (a) Observed annual mean eddy kinetic energy (EKE) in 2016 from AVISO. Simulated annual mean SST in 2016 for LICOM3-HIP at (b) 1°, (c) 1/10°, and (d) 1/20°. Units: cm^2/s^2.

Deleted: **the**

Table 1: Configurations of the LICOM3 model used in the present study.

Experiment	LICOM3-CPU (1°)	LICOM3-HIP（1/10°）	LICOM3-HIP（1/20°）
Horizontal grid spacing	1° (110 km in longitude, approximately 110 km at the equator, and 70 km at mid-latitude)	1/10° (11 km in longitude, approximately 11 km at the equator, and 7 km at mid-latitude)	1/20° (5.5 km in longitude, approximately 5.5 km at the equator, and 3 km at mid-latitude)
Gridpoint	360×218	3600×2302	7200×3920
North Pole	(65°E, 60.8°N) and (115°W, 60.8°N)	(65°E, 65°N) and (115°W, 65°N)	(65°E, 60.4°N) and (115°W, 60.4°N)
Bathymetry data	ETOPO2	Same	Same
Vertical coordinates	30 η levels	55 η levels	55 η levels
Horizontal viscosity	Laplacian A_2=3000 m^2/s	Biharmonic (Fox-Kemper & Menemenlis, 2008) A_4=-1.0×10^9 m^4/s	Biharmonic (Fox-Kemper & Menemenlis, 2008) A_4=-1.0×10^8 m^4/s
Vertical viscosity	Background viscosity of 2×10^{-6} m^2/s with the upper limit of 2×10^{-2} m^2/s	Background viscosity of 2×10^{-6} m^2/s with the upper limit of 2×10^{-2} m^2/s	Background viscosity of 2×10^{-6} m^2/s with the upper limit of 2×10^{-2} m^2/s
Time steps	120/1440/1440 for barotropic/baroclinic/tracer	6s/120s/120s for barotropic/baroclinic/tracer	3s/60s/60s for barotropic/baroclinic/tracer
Bulk Formula	Large & Yeager (2009)	Same	Same
Forcing data	JRA55_do, 1958-2018, 6 hourly	JRA55_do, 2016, daily	JRA55_do, 2016, daily
Integration period	61 years/6 cycles	14 years	14 years
Mixed layer scheme	Canuto et al. (2001, 2002)	Same	Same
Isopycnal mixing	Redi (1982); Gent & McWilliams (1990)	Laplacian	Laplacian

Deleted: about

Deleted: about

Deleted: about

Deleted: A_4

Deleted: /

Bottom drag	$C_b=2.6\times10^{-3}$	$C_b=2.6\times10^{-3}$	$C_b=2.6\times10^{-3}$
Surface wind-stress	Relative wind stress	Same	Same
SSS restoring	20 m/year; 50 m/30 days for sea ice region	Same	Same
Advection scheme	Leapfrog for momentum; two-step preserved shape advection scheme for tracer	Same	Same
Time stepping scheme	Split-explicit Leapfrog with Asselin filter (0.2 for barotropic; 0.43 for baroclinic; 0.43 for tracer)	Same	Same
Sea ice	Sea ice model of CICE4	Not coupled	Not coupled
Ref.	Lin et al. (2020)	This paper	This paper

Table 2: Block partition for the 1/20° setup.

GPUs	$B_x \times B_y$	$imt \times jmt$
384	600×124	604×128
768	600×62	604×66
1536	300×62	304×66
3072	150×62	154×66
6144	100×62	104×66
9216	75×62	79×66
19600	36×40	40×44
26200	36×30	40×34

Table 3: The number calls of halos in LICOM3 subroutines for each step.

Subroutine	Calls	Calls Percentage
barotr	180	96.7%
bclinc	2	1.1%
tracer	4	2.2%

Deleted: halo

Table 4: Some GPU versions of weather/climate models.

Model	Language	Max. Grids	Max GPUs	Year and references
POM.gpu	CUDA-C	1922×1442×51	4 (K20X)	2015 (Xu et al., 2015)
LICOM2	OpenACC	360×218×30	4 (K80)	2019 (Jiang et al., 2019)
FUNWAVE	CUDA-Fortran	3200×2400	2 (V100)	2020 (Yuan et al., 2020)
NICAM	OpenACC	56×56 km×160	2560 (K20X)	2016 (Yashiro et al., 2016)
COSMO	OpenACC	346×340×60	4888 (P100)	2018 (Fuhrer et al., 2018)
LICOM3	HIP	7200×3920×55	26200 (gfx906)	2020 (This paper)

Table 5: Success and failure rates of different scales for one wall clock hour simulation.

GPUs	Success	Failure
384	98.85%	1.15%
1000	97.02%	2.98%
10000	72.90%	27.10%
26200	40.19%	59.81%

Deleted: 1.15%

Page 7: [1] Deleted liu hailong 2021/4/8 AM11:23:00

Page 7: [1] Deleted liu hailong 2021/4/8 AM11:23:00

Page 7: [1] Deleted liu hailong 2021/4/8 AM11:23:00

Page 7: [1] Deleted liu hailong 2021/4/8 AM11:23:00

Page 7: [1] Deleted liu hailong 2021/4/8 AM11:23:00

Page 7: [1] Deleted liu hailong 2021/4/8 AM11:23:00

Page 7: [1] Deleted liu hailong 2021/4/8 AM11:23:00

Page 7: [1] Deleted liu hailong 2021/4/8 AM11:23:00

Page 7: [1] Deleted liu hailong 2021/4/8 AM11:23:00

Page 7: [1] Deleted liu hailong 2021/4/8 AM11:23:00

Page 7: [1] Deleted liu hailong 2021/4/8 AM11:23:00

Page 7: [1] Deleted liu hailong 2021/4/8 AM11:23:00

Page 7: [1] Deleted liu hailong 2021/4/8 AM11:23:00

Page 7: [1] Deleted liu hailong 2021/4/8 AM11:23:00

Page 7: [1] Deleted liu hailong 2021/4/8 AM11:23:00

Page 7: [1] Deleted liu hailong 2021/4/8 AM11:23:00

Page 7: [1] Deleted liu hailong 2021/4/8 AM11:23:00

Page 7: [1] Deleted liu hailong 2021/4/8 AM11:23:00

Page 7: [1] Deleted liu hailong 2021/4/8 AM11:23:00

Page 7: [2] Deleted liu hailong 2021/4/8 AM11:23:00

Page 7: [2] Deleted liu hailong 2021/4/8 AM11:23:00

Page 7: [2] Deleted liu hailong 2021/4/8 AM11:23:00

Page 7: [2] Deleted liu hailong 2021/4/8 AM11:23:00

Page 7: [2] Deleted liu hailong 2021/4/8 AM11:23:00

Page 7: [2] Deleted liu hailong 2021/4/8 AM11:23:00

Page 7: [2] Deleted liu hailong 2021/4/8 AM11:23:00

Page 7: [2] Deleted liu hailong 2021/4/8 AM11:23:00

Page 7: [2] Deleted liu hailong 2021/4/8 AM11:23:00

Page 7: [2] Deleted liu hailong 2021/4/8 AM11:23:00

Page 7: [2] Deleted liu hailong 2021/4/8 AM11:23:00

Page 7: [2] Deleted liu hailong 2021/4/8 AM11:23:00

Page 7: [2] Deleted liu hailong 2021/4/8 AM11:23:00

Page 7: [2] Deleted liu hailong 2021/4/8 AM11:23:00

Page 7: [2] Deleted liu hailong 2021/4/8 AM11:23:00

Page 7: [3] Deleted liu hailong 2021/4/8 AM11:23:00

Page 7: [3] Deleted liu hailong 2021/4/8 AM11:23:00

Page 7: [3] Deleted liu hailong 2021/4/8 AM11:23:00

Page 7: [3] Deleted liu hailong 2021/4/8 AM11:23:00

Page 7: [3] Deleted liu hailong 2021/4/8 AM11:23:00

Page 7: [3] Deleted liu hailong 2021/4/8 AM11:23:00

Page 7: [3] Deleted liu hailong 2021/4/8 AM11:23:00

Page 7: [3] Deleted liu hailong 2021/4/8 AM11:23:00

Page 7: [3] Deleted liu hailong 2021/4/8 AM11:23:00

Page 7: [3] Deleted liu hailong 2021/4/8 AM11:23:00

Page 7: [3] Deleted liu hailong 2021/4/8 AM11:23:00

Page 7: [3] Deleted liu hailong 2021/4/8 AM11:23:00

Page 7: [3] Deleted liu hailong 2021/4/8 AM11:23:00

Page 7: [3] Deleted liu hailong 2021/4/8 AM11:23:00

Page 7: [3] Deleted liu hailong 2021/4/8 AM11:23:00

Page 14: [4] Formatted liu hailong 2021/4/8 AM11:23:00

Font color: Text 1

Page 14: [5] Formatted liu hailong 2021/4/8 AM11:23:00

Font color: Text 1

Page 14: [6] Formatted liu hailong 2021/4/8 AM11:23:00

Font color: Text 1

Page 14: [6] Formatted liu hailong 2021/4/8 AM11:23:00

Font color: Text 1

Page 14: [6] Formatted liu hailong 2021/4/8 AM11:23:00

Font color: Text 1

Page 14: [7] Formatted liu hailong 2021/4/8 AM11:23:00

Font color: Black

Page 14: [7] Formatted liu hailong 2021/4/8 AM11:23:00

Font color: Black

Page 14: [8] Formatted liu hailong 2021/4/8 AM11:23:00

Page 14: [9] Formatted liu hailong 2021/4/8 AM11:23:00

Font color: Text 1

Page 14: [10] Formatted liu hailong 2021/4/8 AM11:23:00

Font color: Text 1

Page 14: [11] Formatted liu hailong 2021/4/8 AM11:23:00

Font color: Text 1

Page 14: [12] Formatted liu hailong 2021/4/8 AM11:23:00

Font color: Text 1

Page 14: [13] Formatted liu hailong 2021/4/8 AM11:23:00

Font color: Text 1

Page 14: [13] Formatted liu hailong 2021/4/8 AM11:23:00

Font color: Text 1

Page 14: [14] Formatted liu hailong 2021/4/8 AM11:23:00

Font color: Text 1

Page 14: [15] Formatted liu hailong 2021/4/8 AM11:23:00

Font color: Text 1

Page 14: [16] Formatted liu hailong 2021/4/8 AM11:23:00

Font color: Text 1

Page 14: [16] Formatted liu hailong 2021/4/8 AM11:23:00

Page 14: [16] Formatted liu hailong 2021/4/8 AM11:23:00

Font color: Text 1

Page 14: [17] Formatted liu hailong 2021/4/8 AM11:23:00

Font color: Text 1

Page 14: [18] Formatted liu hailong 2021/4/8 AM11:23:00

Font color: Text 1

Page 14: [19] Formatted liu hailong 2021/4/8 AM11:23:00

Font color: Text 1

Page 14: [20] Formatted liu hailong 2021/4/8 AM11:23:00

Font color: Text 1

Page 14: [21] Deleted liu hailong 2021/4/8 AM11:23:00

Page 14: [21] Deleted liu hailong 2021/4/8 AM11:23:00

Page 14: [21] Deleted liu hailong 2021/4/8 AM11:23:00

Page 14: [21] Deleted liu hailong 2021/4/8 AM11:23:00

Page 14: [21] Deleted liu hailong 2021/4/8 AM11:23:00

Page 14: [21] Deleted liu hailong 2021/4/8 AM11:23:00

Page 14: [21] Deleted liu hailong 2021/4/8 AM11:23:00

Page 14: [22] Formatted liu hailong 2021/4/8 AM11:23:00

Font color: Text 1

Page 14: [22] Formatted liu hailong 2021/4/8 AM11:23:00

Font color: Text 1

Page 14: [23] Formatted liu hailong 2021/4/8 AM11:23:00

Font color: Text 1

Page 14: [23] Formatted liu hailong 2021/4/8 AM11:23:00

Font color: Text 1

Page 14: [24] Formatted liu hailong 2021/4/8 AM11:23:00

Font color: Text 1

Page 14: [25] Formatted liu hailong 2021/4/8 AM11:23:00

Page 14: [25] Formatted liu hailong 2021/4/8 AM11:23:00

Font color: Text 1

Page 14: [26] Deleted liu hailong 2021/4/8 AM11:23:00

Page 14: [26] Deleted liu hailong 2021/4/8 AM11:23:00

Page 14: [26] Deleted liu hailong 2021/4/8 AM11:23:00

Page 14: [26] Deleted liu hailong 2021/4/8 AM11:23:00

Page 14: [27] Deleted liu hailong 2021/4/8 AM11:23:00

Page 14: [27] Deleted liu hailong 2021/4/8 AM11:23:00

Page 14: [27] Deleted liu hailong 2021/4/8 AM11:23:00

Page 14: [28] Formatted liu hailong 2021/4/8 AM11:23:00

Font color: Text 1

Page 14: [28] Formatted liu hailong 2021/4/8 AM11:23:00

Page 15: [29] Formatted liu hailong 2021/4/8 AM11:23:00

Font color: Text 1

Page 15: [30] Formatted liu hailong 2021/4/8 AM11:23:00

Font color: Text 1

Page 15: [31] Deleted liu hailong 2021/4/8 AM11:23:00

Page 15: [31] Deleted liu hailong 2021/4/8 AM11:23:00

Page 15: [31] Deleted liu hailong 2021/4/8 AM11:23:00

Page 15: [32] Deleted liu hailong 2021/4/8 AM11:23:00

Page 15: [32] Deleted liu hailong 2021/4/8 AM11:23:00

Page 15: [32] Deleted liu hailong 2021/4/8 AM11:23:00

Page 15: [32] Deleted liu hailong 2021/4/8 AM11:23:00

Page 15: [32] Deleted liu hailong 2021/4/8 AM11:23:00

Page 15: [32] Deleted liu hailong 2021/4/8 AM11:23:00

Page 15: [33] Formatted liu hailong 2021/4/8 AM11:23:00

Font color: Text 1

Page 15: [33] Formatted liu hailong 2021/4/8 AM11:23:00

Font color: Text 1

Page 15: [34] Formatted liu hailong 2021/4/8 AM11:23:00

Font color: Text 1

Page 15: [35] Formatted liu hailong 2021/4/8 AM11:23:00

Font color: Text 1

Page 15: [36] Formatted liu hailong 2021/4/8 AM11:23:00

Font color: Text 1

Page 15: [37] Formatted liu hailong 2021/4/8 AM11:23:00

Font color: Text 1

Page 15: [38] Formatted liu hailong 2021/4/8 AM11:23:00

Page 15: [39] Formatted liu hailong 2021/4/8 AM11:23:00

Font color: Text 1

Page 15: [39] Formatted liu hailong 2021/4/8 AM11:23:00

Font color: Text 1

Page 15: [40] Formatted liu hailong 2021/4/8 AM11:23:00

Font color: Text 1

Page 15: [40] Formatted liu hailong 2021/4/8 AM11:23:00

Font color: Text 1

Page 15: [41] Formatted liu hailong 2021/4/8 AM11:23:00

Font color: Text 1

Page 15: [42] Formatted liu hailong 2021/4/8 AM11:23:00

Font color: Text 1

Page 15: [43] Formatted liu hailong 2021/4/8 AM11:23:00

Font color: Text 1

Page 15: [44] Formatted liu hailong 2021/4/8 AM11:23:00

Font color: Text 1

Page 15: [45] Formatted liu hailong 2021/4/8 AM11:23:00

Font color: Text 1

Page 15: [46] Formatted liu hailong 2021/4/8 AM11:23:00

Page 15: [47] Formatted liu hailong 2021/4/8 AM11:23:00

Font color: Text 1

Page 15: [47] Formatted liu hailong 2021/4/8 AM11:23:00

Font color: Text 1

Page 15: [48] Formatted liu hailong 2021/4/8 AM11:23:00

Font color: Text 1

Page 15: [49] Formatted liu hailong 2021/4/8 AM11:23:00

Font color: Text 1

Page 15: [50] Formatted liu hailong 2021/4/8 AM11:23:00

Font color: Black

Page 15: [50] Formatted liu hailong 2021/4/8 AM11:23:00

Font color: Black

Page 15: [50] Formatted liu hailong 2021/4/8 AM11:23:00

Font color: Black

Page 15: [50] Formatted liu hailong 2021/4/8 AM11:23:00

Font color: Black

Page 15: [50] Formatted liu hailong 2021/4/8 AM11:23:00

Font color: Black

Page 15: [51] Deleted liu hailong 2021/4/8 AM11:23:00

Page 15: [51] Deleted liu hailong 2021/4/8 AM11:23:00

Page 15: [51] Deleted liu hailong 2021/4/8 AM11:23:00

Page 15: [51] Deleted liu hailong 2021/4/8 AM11:23:00

Page 15: [52] Deleted liu hailong 2021/4/8 AM11:23:00

Page 15: [52] Deleted liu hailong 2021/4/8 AM11:23:00